B

Periodicals Postage Paid USPS Penton Automatable Poly

ELECTRONIC DESIGN

TECHNOLOGY • APPLICATIONS • PRODUCTS • SOLUTIONS

A PENTON PUBLICATION $8.00 www.elecdesign.com AUGUST 23, 1999

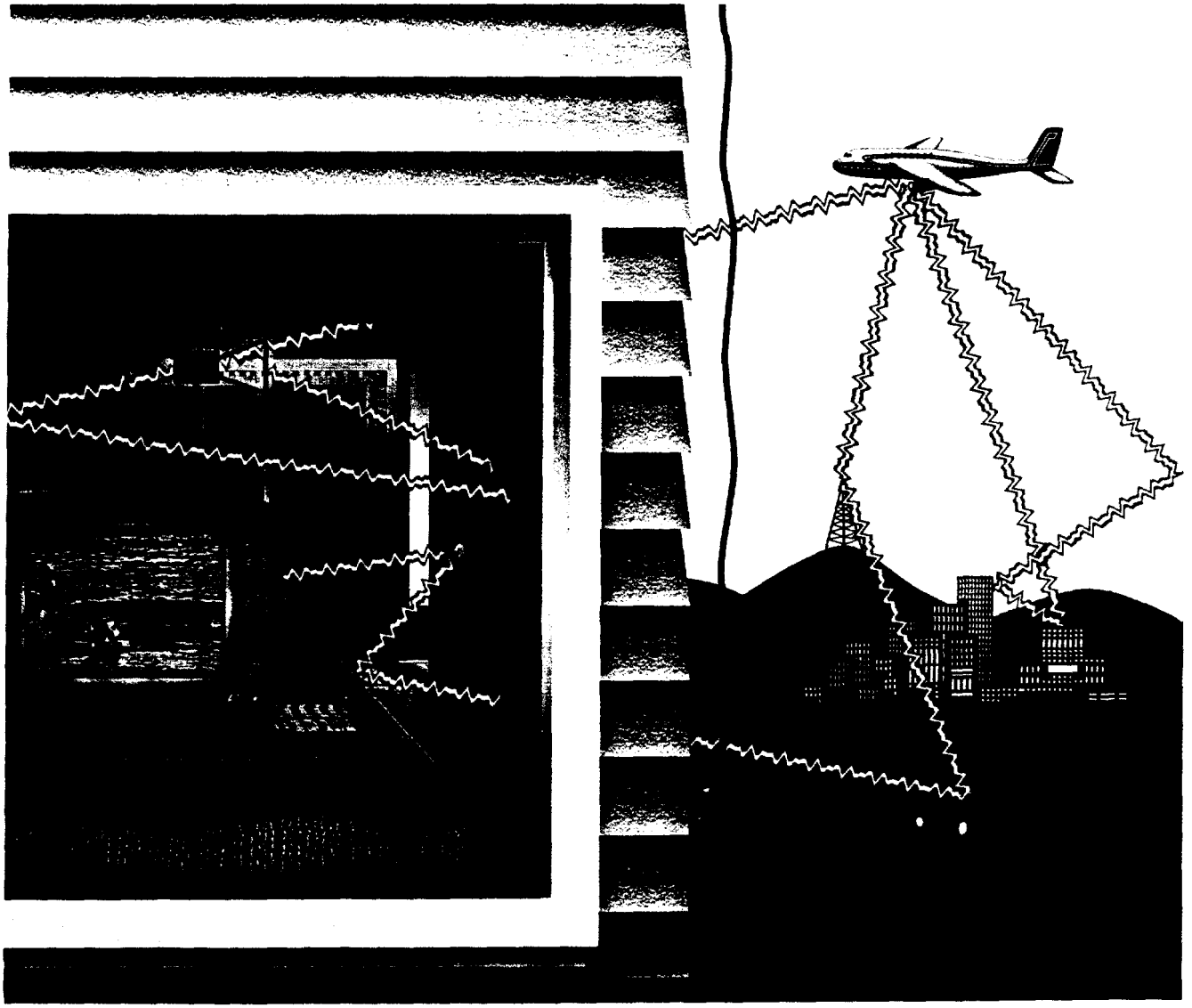

IC Cracks The Code To Improved Digital TV Reception p. 35

TECH INSIGHTS
Developments from the front lines of the communications revolution

VSB/QAM Receiver Cracks The Code To Indoor And Mobile Reception

Using Advanced Blind-Equalization And Acquisition Techniques, This Device Paves The Way To Commercially Viable Digital TV Sets.

Patrick Mannion

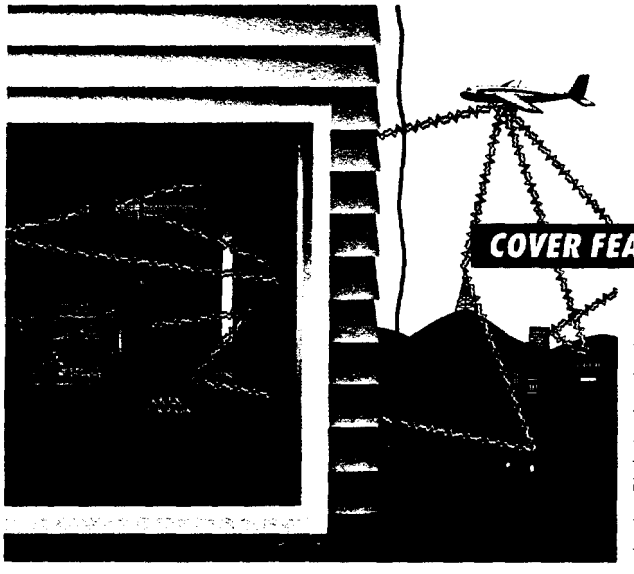

COVER FEATURE

November brings the first anniversary of digital TV's (DTV's) introduction to the mass market. Unfortunately, enthusiasm and hype have slowly given way to a budding realization that serious technical difficulties still exist. These mainly involve the receiver's inability to reliably lock on to the digital signal indoors through a standard antenna. The problems are acute enough to have initiated a groundswell of support for scrapping the current modulation scheme in favor of the European alternative—a move that would render all current receivers virtually useless. Priced between $5000 and $15,000 each, the possibility of such a shift won't be taken lightly by consumers who have already invested their money.

One company is adamant that the current standard's implementation, and not the standard itself, is at fault. NxtWave Communications, Newtown, Penn., has introduced its dual QAM/8-VSB DTV receiver chip. This device appears to have "cracked the code" when it comes to the indoor reception of terrestrial 8-level, vestigial-sideband (8-VSB) DTV broadcasts.

Designated the NXT2000, the chip takes advantage of research into a number of key areas, particularly blind equalization. It mitigates impairments such as static and dynamic multipath interference, phase noise, impulse noise, and adjacent and cochannel interference, all while speeding acquisition time. Tests to date indicate that the chip is fully capable of providing DTV receivers with the ability to quickly acquire and lock on to cable or terrestrial broadcasts in either indoor or mobile (i.e., laptop PC) systems. And it can do so without fear of signal loss due to such everyday occurrences as passing cars, airplanes, or people.

The improvements couldn't have come at a better time. The FCC's DTV broadcast rollout is right on schedule, with up to 30% of the potential market covered as of May of this year. It's essential, then, that the sets be capable of indoor reception if user acceptance is to be expected—not that they haven't already found some acceptance. According to the Consumer Electronics Manufacturers Association's (CEMA's) latest figures, up to 150,000 sets are expected to be in consumers' hands by the end of 1999. Approximately 600,000 more will fly off the shelves by the end of 2000. Extrapolating, CEMA conservatively forecasts that the penetration of DTV sets will reach 30% by 2006, with annual unit sales of up to 10.8 million. To put this in perspective, color TV only rose to 10% penetration in its first eight years, while it took both VCRs and CD players eight years to reach 30% penetration.

While these figures make DTV look good on paper, a number of factors have come into play that may put the kibosh on these predictions. The first of these is cost. The current slew of DTV-receiver offerings are maintaining a price tag way beyond what the mass market can afford. Many of those below $7000 or $8000 need a $1500 (or more) add-on to achieve high-definition-television (HDTV) capability, too.

A number of companies also are finding that average consumers aren't aware of the advantages of digital over analog receivers. Nor do consumers realize the benefits they can expect to accrue from DTV. This is playing havoc with market penetration. As a result, manufacturers are blaming the broad-

casters for not promoting the technology enough. Meanwhile, the broadcasters are passing the buck back to the manufacturers, citing shoddy receiver implementations as the reason for the limited penetration.

The broadcasters may have a point. To date, many purchasers are finding that the only way they can receive a decent signal is by installing a rooftop antenna. They also can pretty much forget about mobile reception. This leads to the third factor, which is whether or not the right modulation scheme was chosen for terrestrial broadcasting to begin with—at least for the North American market, anyway.

There are two very different digital-modulation techniques being used in digital-television terrestrial broadcasting (DTTB). One is the trellis-coded 8-VSB scheme developed by the Grand Alliance (GA) and endorsed by the Advanced Television Systems Committee (ATSC). The other is the coded orthogonal frequency-division multiplexing (COFDM) design adopted in the Digital Video Terrestrial Broadcasting (DVB-T) standard. A derivative of the COFDM, the bandwidth-segmented transmission (BST) OFDM system is currently being finalized in Japan.

Since there's more than one option, many countries and administrations are busy considering the optimum standard for their parts of the world. Criteria being used in the selection process include spectrum resources and policy, coverage requirements and network structure, reception conditions, type of service desired, program exchange, cost to the consumers, and broadcaster requirements.

COFDM was chosen for Europe, and more recently for Australia. In North America, 8-VSB was selected for a number of reasons. Primarily, it's more robust in an additive-white-gaussian-noise (AWGN) channel. It also has a higher spectrum efficiency and a lower peak-to-average power ratio. And, it's sturdier in the face of impulse and phase noise. All of these make it suited to the widely spread-out, electronically noisy market to which it is being applied.

While COFDM has a number of advantages, one of the key areas in which it excelled from the beginning was in its ability to deal with dynamic, multipath distortion (DMD). Deriving from multiple signals bouncing off swaying buildings and towers, along with overhead aircraft and passing cars—even people walking within the room—DMD is the main hurdle on the way to clear, indoor-antenna or mobile reception of digital data. This one factor alone has companies such as Sinclair Broadcasting, Baltimore, Md., calling for the axing of the 8-VSB scheme in favor of COFDM.

The furor started last year. Engineers at Sinclair, owner of 13 stations that must begin digital broadcasting according to the FCC timetable, found that they could not reliably receive a viewable digital picture within the confines of city buildings. Yet defenders of the 8-VSB system, which include GA members that invented the scheme, insist that Sinclair's tests were faulty. They believe the engineers not only slanted the tests in favor of COFDM, but also used first-generation 8-VSB implementations, which are widely known to be unsatisfactory in the light of newer introductions.

One of the chief supporters of this "first-generation" stance is NxtWave Communications. This firm now offers its NXT2000 ATSC-compliant decoder as the solution to the problems Sinclair and other broadcasters and customers are experiencing.

Along with multipath capability, one of this device's key features is its ability to use the same core to decode both 8-VSB terrestrial and cable signals, such as 16-VSB and SCTE DVS-031-, ITU-J.83B-, and MCNS DOCSIS-compliant 64/256 QAM. All that's needed to select between the two are control bits from the I^2C control bus. Other features include direct IF sampling, an equalization range of –4.5 to 44.6 μs, and an acquisition time of under 50 ms. Based on 0.25-μm technology, the chip operates off 2.5 V at the core and 3.3 V at the peripheral. Power requirements are expected to be in the 1-W range, which is much better than the 3 to 4 W demanded by current devices.

To understand more clearly how NxtWave became the first company to achieve reliable indoor reception, it's helpful to take a closer look at the block diagram *(Fig. 1)*.

The input to the all-digital chip is either a 44-MHz IF or the 6.28-MHz baseband. This feeds the 10-bit analog-to-digital converter (ADC), which is controlled by a free-running (FR) clock operating at 25 MHz. The use of an FR clock, as opposed to a voltage-controlled crystal oscillator (VCXO), means that some kind of interpolation is necessary later on in the circuit to resample the data.

Still, the method has its advantages. The extended delay in the phase-locked loop (PLL), caused by forcing the clock in the ADC to be at the correct frequency, is avoided. Eliminating the VCXO also saves on-board real estate, improves device temperature stability over time, and greatly reduces imple-

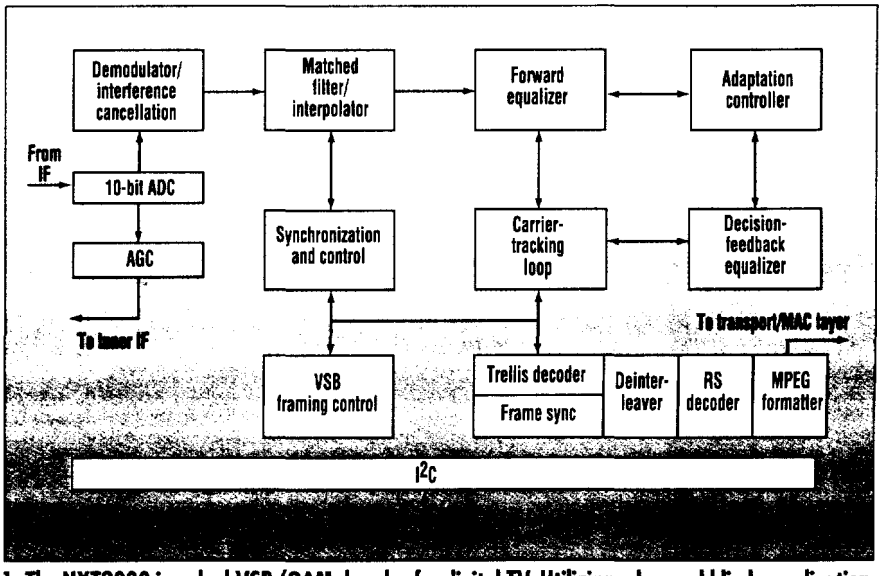

1. The NXT2000 is a dual VSB/QAM decoder for digital TV. Utilizing advanced blind-equalization and acquisition techniques, the chip is the first 8-VSB decoder to achieve fast and reliable indoor and mobile reception of terrestrial broadcasts using a standard bow-tie antenna and tuner.

mentation costs. Additionally, the FR clock simplifies the QAM/VSB switching process. A programmable automatic-gain-control (AGC) circuit tunes the dynamic range of the input signal.

The ADC's output is supplied to the demodulator. This includes a phase splitter to create a complex baseband signal and its corresponding I (in-phase) and Q (quadrature) symbols. Also, the demodulator has an interference canceller that has completely programmable coefficients. These let the system effectively cancel adjacent or cochannel interference—namely the NTSC signals—which are of significantly higher power. The cancellation algorithm is key to this operation. As a result, it remains proprietary.

The demodulator output then feeds a combined matched filter and interpolator. The interpolator resamples the data according to a programmable numerically controlled oscillator (NCO). In turn, this is governed by a PLL driven by an integrated timing phase detector. The PLL is fully programmable, and it's automatically tuned during the acquisition process. The matched filter provides out-of-band rejection. It's also matched to the transmitter pulse-shaping filter for both QAM and VSB signals. The output then goes to the equalizer—the key to the whole operation.

Combined carrier recovery and equalization is essential for robust and reliable demodulation of heavily impaired digital TV signals. Furthermore, it has been well established that a decision-feedback equalizer (DFE) provides near-optimum error-rate performance with low complexity and implementation cost. The DFE is a feedback loop that feeds back hard decisions (quantized "best guesses") to additively cancel the intersymbol interference (ISI). If there are a lot of errors, the loop can be unstable. The key to making this loop work is to remove as much of the error as possible.

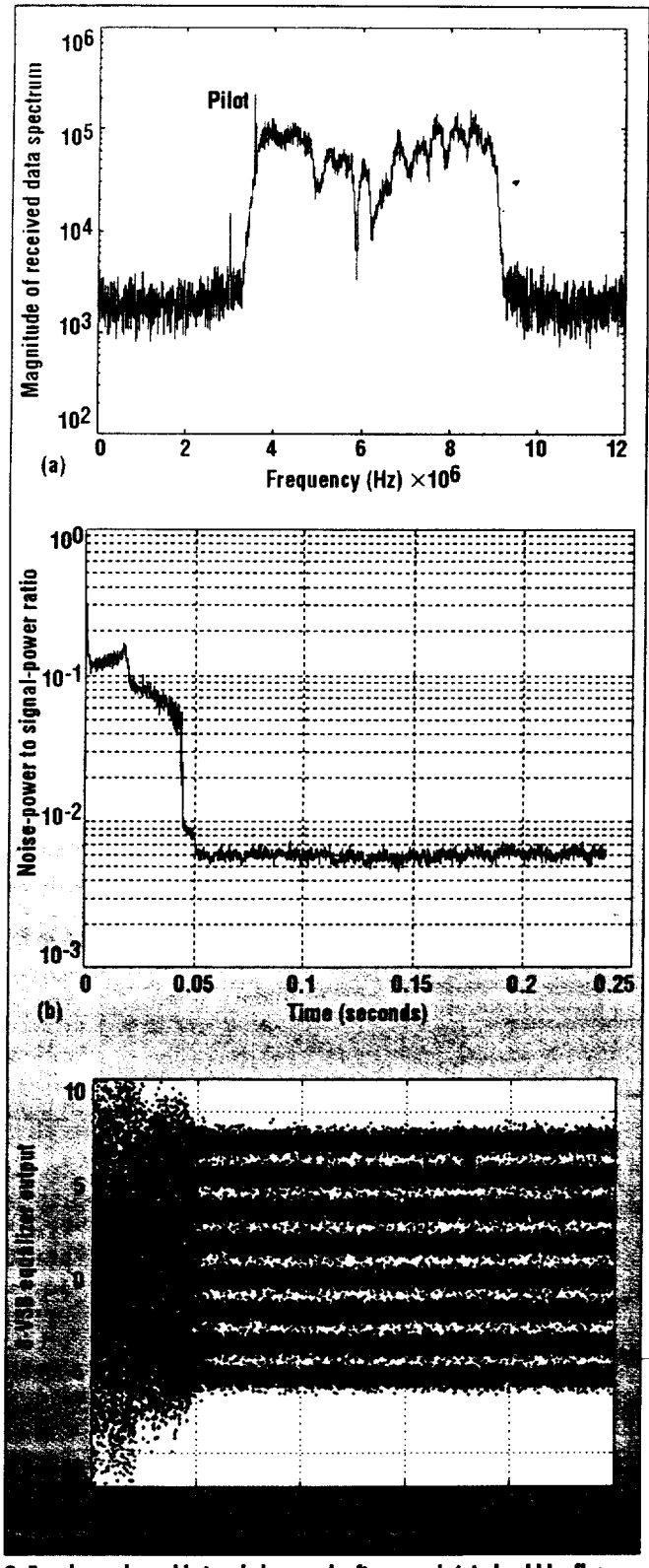

2. For the real-world signal shown, the first graph (a) should be flat across the band, with no distortion. Note the pilot tone. But multipath-induced distortion causes spectral degradation of more than 20 dB. The second graph (b) clearly reveals that within 50 ms, the output goes from a closed-eye to an open-eye setting, and the error is reduced to about 23 or 24 dB. The last graph (c) illustrates the eight distinct levels of the VSB output of the equalizer over time.

Realistic signaling environments prohibit cold-start initializations of DFEs, because high error rates prevent reliable decisions. They also can cause equalizer divergence. The ATSC recognized this and embedded a training sequence into the VSB format to aid equalizer and carrier acquisition. During acquisition, equalizer adaptation typically is completed solely with the training sequence. But the sequence isn't transmitted very frequently (every 24 ms), which translates into extremely slow equalizer convergence. In the presence of rapidly time-varying channels, the training-sequence rate is so slow compared to the channel variations that equalizer convergence is prevented. It's essential to note that the indoor- and mobile-channel characteristics both exhibit rapid time variations.

To get around this problem, the NXT2000 uses NxtWave-proprietary algorithms. This accomplishes blind initialization of a DFE without precise carrier lock. It also does so in the presence of closed-eye impairments.

A linear infinite-impulse-response (IIR) structure that doesn't require symbol decisions is used during the initial acquisition phase. A proprietary modification of the constant modulus algorithm (CMA) is employed to update the equalizer coefficients at every symbol instance during this blind startup. Since the CMA doesn't depend on the signal's phase, the carrier loop is coarse-tuned during acquisition. The CMA's modification is statistically based. It uses reduced-precision update rules to decrease multi-

plier chip area. After acquisition, the linear IIR loop is transferred to the nonlinear DFE structure. Decision-directed updates are then used in place of the CMA updates. The transfer is automatically accomplished using proprietary control algorithms.

To further enhance the reliability of symbol decisions used in the DFE with decision-directed updates, the device exploits a proprietary algorithm. This allows efficient joint trellis decoding and equalization with low signal latency, which is essential here. While it's well known that better decisions can be made with a trellis decoder, by the time those decisions are fed back in a typical system, they're too old to be of much value. The joint trellis decoding and equalization, with low signal latency, is commonly called maximum-likelihood sequence estimation (MLSE).

The terrestrial TV channel regularly has reflections up to a delay of 45 μs. For the 10.76-Mbaud data rate, this translates into approximately 500 equalizer coefficients (taps). Generally, the channel is "sparse." Most channel energy is centralized into clusters so that many channel coefficients are near-zero. The NXT2000 uses an adaptive-allocation algorithm that places a subset of taps across 528 positions. This subset contains much fewer than 528 taps, thereby saving greatly on processing (complex multiplies). The location of the active subset of taps among the possible 528 positions is done adaptively. Hence, the tap-allocation algorithm senses channel time variations and re-allocates the active taps across the 528 positions. The result is extremely fast tracking capability with low adaptation jitter, relative to nonadaptive techniques.

Nonadaptive techniques solve for a channel estimate first. Based on that estimate, they decide which taps to make active. Those selected are then permanently set, regardless of channel changes. Worse again, some implementations may activate all 528 taps, with their corresponding complex multiplies. This slows down the decision process and adds greatly to both device cost and silicon real estate.

All of the above signal-processing operations are implemented in an architecture that allows for nearly complete reuse of gates between VSB and QAM signaling formats. The combination of NxtWave-proprietary timing and carrier recovery, equalization, and decoding techniques results in a receiver with an acquisition time that is usually less than 50 ms *(Fig. 2a, b, and c)*. The plots shown were made indoors with a bow-tie antenna and a real-world tuner. The transmitter was located approximately 35 miles away (Channel 26, out of Philadelphia).

The first graph *(a)* should be flat across the band, with no distortion. But multipath-induced distortion caused severe spectral degradation—more than 20 dB. The second *(b)* clearly shows that within 50 ms, the output goes from a closed-eye to an open-eye setting, and the error is reduced to about 23 or 24 dB. The last one *(c)* displays the eight distinct levels of the VSB output of the equalizer over time. The first 50 ms are muddled and completely closed eye.

The bottleneck in this 50 ms is usually the forward-error-correction (FEC) synchronization. It requires the detection of the embedded training sequence that's sent every 24 ms. While this delay may appear to make the whole blind-equalization and rapid-acquisition process all for nought, such is not the case. Though

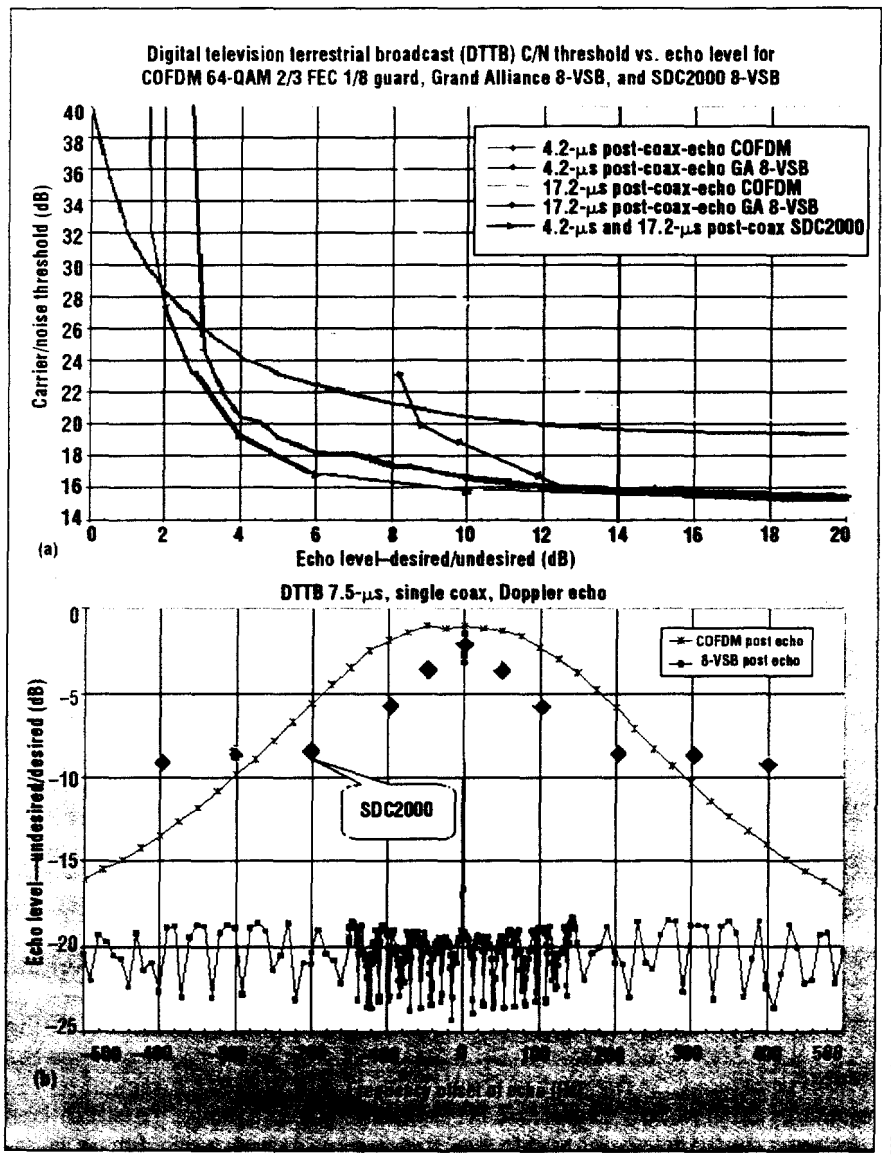

3. Static (a) and dynamic (b) multipath performance curves expose how well the SDC2000 has bridged the gap between VSB and COFDM. The only area where COFDM exceeds the SDC2000 is in the unrealistic scenario where the receiver is situated exactly between two transmitters. Yet the SDC2000 really shows its strength in the dynamic curve.

the system is still dependent upon the timing sequence, it doesn't have to wait for eight or 10 training sequences, which is typical of trained-equalization implementations. Here, the system can perform the equalization within one or two frames, and then just wait for one sequence to lock up the FEC—and it's done. Another key aspect is acquisition. In a changing channel environment, once the system has locked onto the FEC synchronization, it's always locked on. The FEC subsystem implements both ATSC and J83b standards.

The static- and dynamic-multipath performance curves also are shown, *(Fig. 3a and b)*. Done in Australian labs that compared the GA system with COFDM, these graphs (minus the NXT2000 version) caused the labs to go with COFDM over VSB. The figure illustrates how well the NXT2000 has bridged the gap. In some places, it even outperforms COFDM.

Take Figure 3a. Ideally, there would be a flat—not curved—line corresponding to y = 15 dB. This would imply that as the impairment coming into the system is increased, the carrier/noise threshold doesn't degrade at all. In a real-world situation, unfortunately, there is some degradation—the amount of which is dependent upon the system.

The NXT2000 forms the lower envelope of all the curves up until around 1.8 dB. This means it's better than COFDM for long echoes, while close-in echoes favor COFDM. The NXT2000 is better than all the echoes which are less than 2 dB. The only area where COFDM exceeds the NXT2000 is in the unrealistic scenario where the receiver is situated exactly between two transmitters.

The NXT2000 really shows its strength in Figure 3b. Usually, if a vehicle is moving at about 50 mph, a frequency offset of about 100 Hz can be expected. NxtWave also has noticed that in an indoor environment, the offset is often up to 15 Hz. COFDM has a pretty robust performance up to about ±100 Hz. Then, it dies out and is about 15 dB down at 500 Hz. The 8-VSB signal degrades pretty drastically for the GA system. Within 5 Hz, it's almost 20 dB down. COFDM is still better than VSB, but not substantially so. At 100 Hz, it's only about 3 dB up. If the echo delay is more than 7.5 µs, the NXT2000's performance improves. As mentioned before, the delay depends on the environment. It's possible to get very strong echoes with very long delays. ❐

C

ADVANCED IMAGING
Solutions for the Electronic Imaging Professional • September 1999

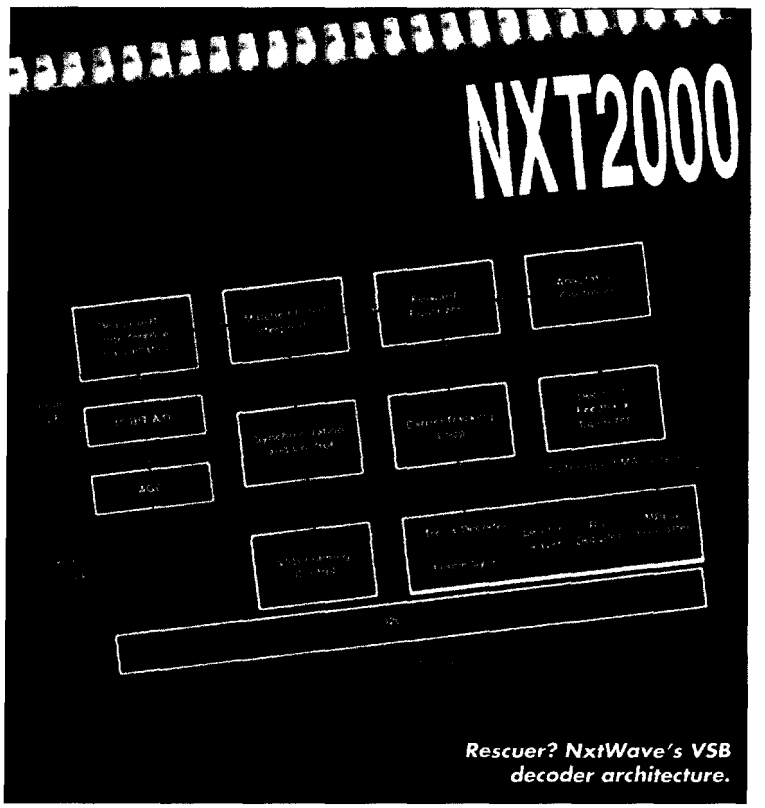

Rescuer? NxtWave's VSB decoder architecture.

Beyond the Transmission Controversy:

Digital Television's New Datacasting Future

By Richard Doherty

EVERYONE HAS HAD AN AXE TO GRIND—ON TWO CONTINENTS. WHETHER THERE'D EVEN BE A DTV TO IMPROVE WAS IN QUESTION. BUT SMARTER CHIPS APPEAR TO HAVE COME TO THE RESCUE.

Almost incredibly, for many months this year, the very future of Digital Television—and its premium flagship service, HDTV—seemed in doubt of a sustainable U.S. rollout.

This summer, Sinclair Broadcasting, the largest independent owner of TV stations (many associated with leading broadcasters, others as independents) petitioned the Federal Communications Commission to scrap the present Digital TV modulation scheme (Vestigial Side Band, or VSB) in favor of a European method (COFDM) which would not suffer from reception problems due to multipath ghosts and signal impairments in the inner cities—conditions which many Sinclair stations have been experiencing.

Starting in the spring of 1999 (for as-yet-unknown reasons), Sinclair engineers began calling together the most easily-impressed editors of the broadcasting business infrastructure to tell them that the FCC's choice for digital transmitter modulation was flawed and that, in fact, VSB was so flawed that the FCC should immediately reverse the mandatory rollout of Digital TV and instead choose the COFDM data modulation scheme that is now popular in Europe. Sinclair engineers arranged demonstrations using $5 to $15 UHF bow-tie antennas in parking garages; places where their opponents snidely commented that no analog set could even receive a signal. They were also using first-generation VSB tuners and second-generation COFDM decoders, raising questions of a lack of parity.

To all the makers of high-quality digital and HDTV broadcast and production equipment, including transmitter and studio equipment suppliers, and to the consumer electronics manufacturers delivering initial HDTVs and DTVs, the Sinclair technical challenge was *absolutely the last thing that anyone wanted to happen.*

CEMA, the Consumer Electronics Manufacturers Association, quickly blasted Sinclair for not raising this concern three years ago during the appropriate technology review window. Rival station owners speculated that Sinclair was simply trying to put off the (expensive) legal commitment to modify their station studios and transmitters. Still others linked Sinclair's sudden effort with an expression by **Microsoft** senior management that VSB was too flawed to serve future portable broadcast data reception needs.

Smarter decoder chips to the rescue

Instead of rolling over and playing dead, this time, engineers from leading semiconductor companies and architects of the HDTV/DTV system itself have rolled up their sleeves and begun to show solutions which not only defuse Sinclair's concerns, but also deliver reception robustness undreamt of by the original ATSC VSB systems architects.

In late August, both **Motorola** and Sarnoff spin-off **NxtWave Communications** (Newtown, PA) announced smart VSB decoder chips which, when integrated into PC tuner cards, set-tops and Digital TVs this fall and winter, squash most of Sinclair's concerns.

Motorola is a leading supplier of COFDM decoder silicon in many markets and knows the nuances of its robust, real-time decoding very well. So when Motorola Semiconductor licensed key VSB technologies from ATSC system co-inventors at **Sarnoff Labs** (Princeton, NJ), they knew that they would need to mesh Motorola's special skills in digital signal processing, fast symbol decoding and error correction with Sarnoff's insight.

The result is now a commercial part of Motorola's

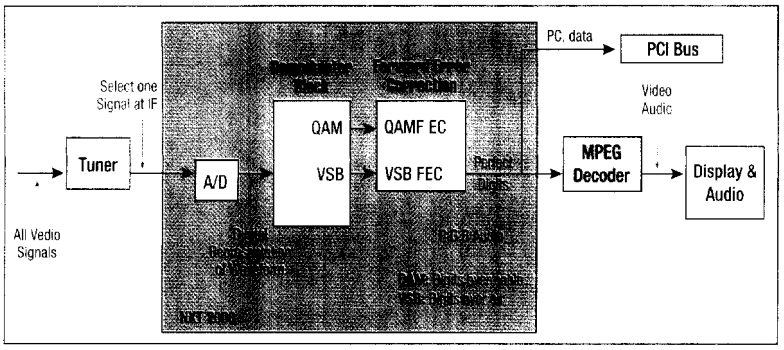

NxtWave's multi-format receiver's operation.

Digital DNA family of HDTV and DTV chips and chip set solutions. The MCT2100 is being tested in moving vehicles, offices, and living rooms in many "problem" DTV cities on the east coast, and is doing quite nicely, according to Motorola engineers we spoke with in August.

Within a day of the Motorola announcement, **NxtWave Communications** combined their expertise in decoding both VSB and QAM (Quadrature Amplitude Modulation) on a chip which should allay consumers' set-top fears when attaching to both antenna and cable DTV sources. NxtWave's technical team hails from both Sarnoff itself and **General Instrument**'s cable box Jerrold division in nearby Hatsboro, PA.

As a fabless design house, NxtWave is tapping **STMicroelectronics** for their first silicon. Like Motorola, their engineers believe that they have not only tackled (and won in) boosting the ability to decode VSB in the inner city, but also ensured that deep suburban household reception is equally well received, just as the architects of VSB at Zenith engineered.

Looking back to the FCC decision point

COFDM, VSB and QAM were all considered for the North American Digital TV/Advanced Television Systems Committee standard. VSB won out for a variety of reasons.

Vestigial Side Band was viewed as a godsend when the RF experts and digital engineers at **Zenith Electronics** first disclosed it at the beginning of the '90s. First, by going to 8 VSB (higher symbol levels) the entire 19.3-megabit payload of HDTV, audio and accompanying data services could be squeezed into a 6 MHz RF channel. Next, VSB was relatively simple to decode, important to jump-starting their nascent HDTV and Digital TV industry, then seen as less than five years away.

Most importantly, VSB solved both the audience-reach and adjacent-channel problems. NTSC viewers would simply see noise on a VSB channel as they tune past, yet that noise was a fully-encoded Digital TV program set. And, by operating at lower powers than Amplitude Modulated TV and its accompanying FM sound carrier transmitter, broadcasters could get both at a nearly equivalent transmitter reach and do it at less power.

Zenith is also beginning to deliver their second-generation professional tuners and first consumer products using second-gen VSB technology. At press time, Zenith economic fiscal restructuring prevented their management or engineers from commenting directly. However, suffice it to say that the next-generation VSB decoder and remodulator chips shown at the national Cable TV Show in late spring were both more sensitive to fringe reception and handling inner-city and close-suburban reception than their initial (excellent-quality) DTV VSB tuners.

While many critics maintain that the then-cash-strapped ATTC (Advanced Television Test Center) needed to scale back the number of cities and varieties of terrain tested with VSB, it nonetheless did the job and allowed the FCC to approve the system in late December 1996.

Serving a different landscape

At the same time, early adopters of digital television in Europe were serving *a different broadcast audience entirely*. Most viewers in Europe are in the close-in cities. TV transmitters that match the power and antennas that match the height of most U.S. cities are rare, so Coded Orthogonal Frequency Domain Modulation, or COFDM, became the system of choice.

Sinclair's FCC tests used a low-power transmitter in Baltimore. As many broadcast engineering trade journals and Web sites will reveal, COFDM was designed for European 8 MHz channel spacing. Without care, a great deal of adjacent NTSC channel interference ("splatter") might result in the U.S.' 6 MHz spacing environment. Also, COFDM-6 results in a data rate a few megabits shy of the 19.3 Mbit/sec payload expected for the ATSC system.

So, at the same power levels, COFDM also carries slightly less data, and VSB proponents say that up to 6 dB of additional transmitter power would be needed to reach the same audience distances as viewers now enjoy for analog. To metro New York, that means COFDM (at the same power as VSB) might lose between five and six million viewers in the suburbs.

VSB works over cable

Note that one early dismissal of the Sinclair challenge was that as the vast majority of inner-city households receive, at best, poor analog TV reception (instead opting for cable or satellite) the multipath weaknesses of initial VSB tuners were rather moot. Most owners who could afford DTV would scrap the $5 UHF bow-tie antenna that Sinclair was using and either opt for cable or satellite signal access. And, while cable companies initially resented the need to "must carry" ATSC stations' VSB signals, opting instead for more (cable) robust QAM instead, recently, two cable companies have shown that VSB modulation is up to that task as well.

VSB can also be used to deliver digital broadcasts over cable TV, such as in Manhattan Cable in New York City and Cablevision Systems (which serves 3.4 million customers in the Metro New York region). By using VSB modulators over the existing cable plant, VSB allows the existing tens of thousands of HDTV receivers to deliver Home Box Office HD and show high-definition feeds of Madison Square Garden hockey, basketball and special events, as well as live New York Mets' and New York Yankees' baseball games.

These sports and entertainment venues also happen to be owned by Cablevision Systems. Indeed, Cablevision hopes to provide these services and others—such as the Radio City Music Hall Christmas Show—to other cable TV systems this winter via satellite, joining their rainbow programming properties which now deliver AMC, Bravo and the Independent Film Channel to cable and satellite households.

Getting better all the time...

Engineers at Motorola, NxtWave, Zenith and Sarnoff have all expressed their confidence that the ability to encode, transmit and deliver VSB will continue to grow. Today, mobile data reception in moving vehicles and the ability to move receivers all about the home are the prime benefits. Tomorrow, the ability to enjoy VSB data reception on hand-held devices may even be in the offering, allowing every TV stations to become a mobile, personal datacaster as well.

Indeed, Zenith believes so strongly in VSB that they have also developed 16-VSB chips which decode existing 8-VSB signals and new higher-data-density modulation as well. These 16 VSB chips are capable of decoding the same 39.7 Mbits/sec of data as cable TV's 256-QAM. Shown to the industry for several months, Zenith managers now envision 16-VSB remodulators being used for a coaxial-cable-based home RF network. By re-modulating up to two 8-VSB signals and packing two HDTV (or DTV multicast) channels into the space of one, personal A/V and data distribution is possible using ordinary room-to-room coax.

This data transmission is feasible over a closed-loop indoor cable distribution in the home, whereas 16-VSB is not yet suitable for over-air transmission. It would allow next-generation set-top boxes and VCRs to receive, decode and then remodulate HDTV and Digital TV signals for reception throughout the home, and could also carry a 20-MBit data network in addition to a single HDTV signal.

In the coming months, at least one other improved chip decoder is expected to be announced, and by this winter, their use with new so-called smart antennas may have Digital TV owners—and set-top box users—rejoicing as they receive ghost-free pictures, sound and data services that were previously impossible on their ancient analog predecessors. ■

Electro-physicist Richard Doherty, a frequent contributor to *Advanced Imaging*, directs both advanced digital products and services technology testing and market research at The Envisioneering Group (Seaford, NY). He can be reached at *rdoherty@envisioneering.net*.

Reprinted with permission from the publisher of the September 1999 edition of *Advanced Imaging*.

For subscription information, please call 920-563-1769, or fax us at 920-563-1704.

D

Feasibility of Reliable 8-VSB Reception

C.H. Strolle, S.N. Hulyalkar, T.J. Endres
NxtWave Communications
One Summit Square
Doublewoods Rd.
Langhorne, Pa. 19047

Abstract

This paper discusses insights into the Vestigial Sideband (VSB) modulation format and advanced demodulation techniques that can be utilized to provide reliable 8-VSB terrestrial reception. VSB is a special form of amplitude modulation that maintains a small portion of the undesired (or redundant) sideband, often called a vestige. VSB has a long history and wide application in analog communications and is particularly useful for digital communications since it can be shown to be equivalent to a special form of QAM called Staggered QAM (SQAM). In the SQAM signal, the quadrature component of the QAM signal is delayed by T/2 (baud rate T) with respect to the in-phase component of the QAM signal. Our paper will illustrate the equivalence between 8-VSB and 64-SQAM. This equivalence is significant since many of the synchronization and equalization techniques that have been developed for QAM signals will be shown to be feasible for the reception of 8-VSB HDTV signals.

VSB as SQAM

The equivalency of 8-VSB to 64-SQAM can be readily established in the following way. Referring to Figure 1, 8-VSB is initially represented as a real valued 8-PAM signal. After the negative portion of the spectrum is removed by creating a complex valued signal in which the quadrature component is converted to the Hilbert Transform of the in-phase component, the signal is then spectrally shifted by -f(s/4), where "s" is the VSB symbol rate, to establish a baseband SQAM signal in which each component (I and Q) contains half the information of the original 8-VSB signal. The resulting symbol period for each component is twice that of the original VSB signal, although the Q channel symbols are delayed ½ of a symbol period from the I channel symbols.

Second and Third Generation Receiver Design

Newer generation receivers that utilize the equivalency between VSB and SQAM typically contain the processing blocks illustrated in Figure 2. Double lines indicate complex (I and Q) signal processing paths.

Tuner: The three main requirements for a terrestrial DTV tuner are a low noise figure, relatively low phase noise and immunity from signal compression. A noise figure of 7dB or less that is uniform across both the VHF and UHF tuning band is necessary. A low noise figure is required when operating in fringe areas and when receiving signals with indoor antennas where both multipath and weak signal conditions exist. Phase noise of –80 dBc or less at 10 kHz is also desirable. A lower phase noise of –85 dBc has added benefits since it allows the carrier tracking loop to operate with a lower loop bandwidth and gain, slightly improving gaussian noise performance. Immunity from compression is needed when attempting to receive weak signals that are located (spectrally) near strong adjacent NTSC signals. As the AGC system adjusts for the weak DTV signal, the tuner tends to go into compression since it is simultaneously amplifying the strong signals as well.

IF/SAW Processing: The main requirement for the IF system is sufficient removal of adjacent channel components and IF gain of 60dB or greater. Currently most receivers utilize two stages of SAW filters (designed for cable applications) to obtain the desired adjacent channel rejection.

Demodulator: This block takes a real signal and converts it to a baseband or near baseband complex signal. Some first generation receivers and the ATSC reference system (Zenith Blue Rack) utilize a synchronous demodulator where

NAB 2000 (Las Vegas)

Figure 1

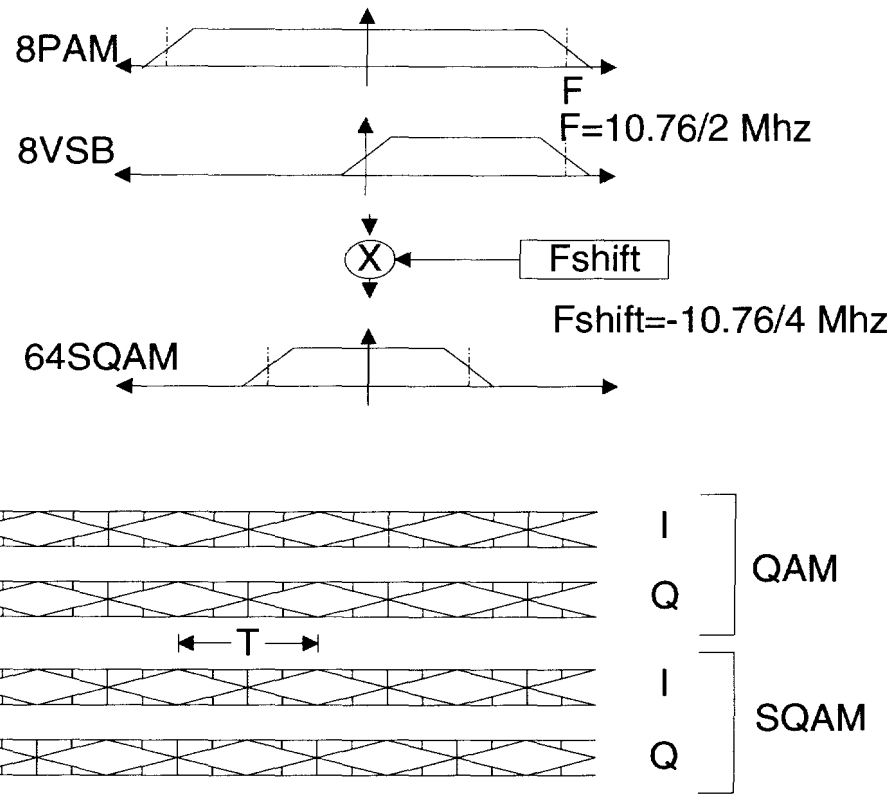

QAM { I(t),Q(t-T/2) }=SQAM{ I(t),Q(t) }

8VSB= Fshift{ 64QAM { I(t),Q(t-T/2)}}

only the real (in-phase) component is processed. Significant performance degradation occurs when quadrature multipath components are present or the pilot signal is attenuated or even lost. In these cases a severe burden is placed on the equalizer by forcing it to phase rotate the entire signal by performing a Hilbert Transform. These problems can be completely avoided by processing the quadrature component.

AGC: The signal for the agc is usually derived directly after the A/D converter to ensure that the signal level is within the conversion range of the A/D. When strong co-channel or strong residual adjacent components are present, the AGC system must compensate for this and attenuate the signal at the A/D and then boost the desired component after the undesirable components have been removed.

Interference Cancellation: A significant performance increase over first generation receivers can be obtained when receiving signals with co-channel or strong adjacent channel NTSC interference by filtering with tunable notch filters. These receivers and the ATSC reference system utilize a 2-tap comb filter to remove the co-channel components. When the comb is engaged, the gaussian noise performance degrades by 3dB. Furthermore, when the comb is engaged, the trellis decoder must switch to a sub-optimum 8-state partial response trellis decoder. This can all be avoided by employing low loss notch filters at the video and audio carriers and allowing the DFE to cancel the ISI created by the notch filters. The loss created by this method is .5dB or less and the trellis decoding can remain as a 4-state decoder. Additionally, since the notches are programmable, co-channel and adjacent channel rejection is easily implemented for an 8 MHz

Figure 2

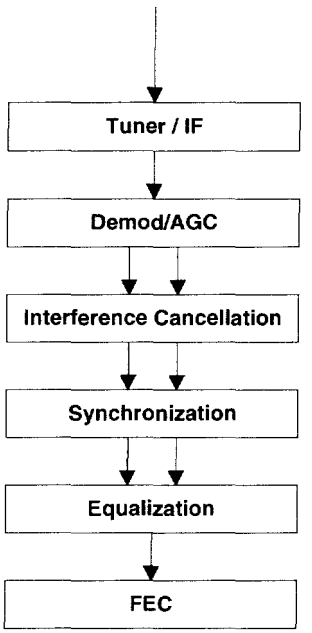

VSB system, increasing the applicability of the ATSC format throughout the world.

Synchronization: Baud recovery or symbol recovery can be achieved in a variety of ways. Some first generation receivers and the ATSC reference system utilize a segment sync detector circuit similar to a line locked clock found in a television receiver. In these implementations the timing phase detector operates on pre-equalized segment sync symbols that rely exclusively on a synchronous demodulator and therefore are vulnerable to pilot loss and quadrature multipath. Newer implementations borrow from the various techniques available from QAM receiver design. Primarily they fall into two classes: decision directed [1] or band edge timing [2]. Band edge timing has the advantage that it can be independent of carrier offset and can be situated prior to carrier recovery. The decision directed method has the advantage that it operates on the post equalized symbols and utilizes the broadband signal energy. Both methods tend to be very robust since they are tracking a very stable reference at the transmitter and therefore the loop bandwidths can be very narrow, providing excellent immunity from channel impairments.

In direct contrast to symbol timing recovery, the carrier recovery system needs to track an unstable reference primarily due to the phase noise inherent in the tuner. This requires that the loop bandwidth of the carrier tracking loop be sufficiently wide to track the tuner phase noise. This is a particular problem in first generation receivers which rely on the pilot loop alone to perform carrier frequency and phase tracking and for receivers that rely on the pilot to perform frequency tracking and use a first order phase tracking circuit to perform fine phase adjustments. In either situation, significant degradation is encountered when dynamic multipath is present in which the pilot is undergoing significant amplitude and phase rotations. In these implementations, the equalizer and phase tracker need to respond to the phase rotations introduced by the pilot loop itself, severely reducing their effectiveness in combating the multipath. Again, borrowing from QAM receiver design, one can simply ignore pilot aided carrier recovery methods (and the resulting degradation it introduces) and employ a second order decision directed carrier recovery loop.

Equalization and Carrier Tracking: Numerous architectures are available for use in the VSB equalizer, all of which can be traced directly or indirectly from QAM equalizers. In addition, many techniques are available for updating or adapting the equalizer coefficients to compensate or remove the ISI created by multipath. Table 1 illustrates the various options available and Figure 3 illustrates the architectures implied by these options.

TABLE 1

Type	Forward Section	Feedback Section	Complexity
I	Baseband/Real	Baseband/Real	Low
II	Passband/Half Complex	Baseband/Real	Medium-Low
III	Baseband/Full Complex	Baseband/Real	Medium-Low
IV	Passband/Full Complex	Baseband/Real	Medium
V	Passband/Full Complex	Passband/Half Complex	High

Figure 3

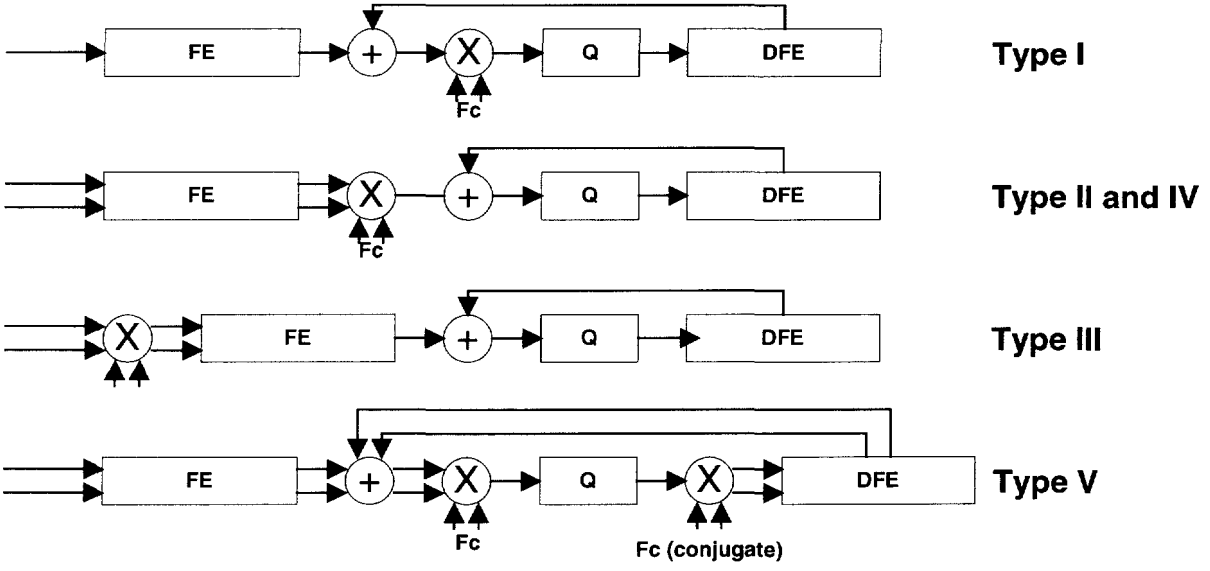

Type I processes only the real (in-phase) component and the coefficients are real valued. This architecture is found in the ATSC reference system and many first generation receivers. Since there is no quadrature component, the phase tracker must regenerate an approximation of the Q component as shown in [3]. The phase tracker in this case is useful for only small phase errors, however when large errors are present, quadrature distortion remains. This structure is particularly susceptible to pilot corruption and quadrature multipath. The DFE for the first four structures is the same. Type II processes both the in-phase and quadrature components with real valued coefficients and generates in-phase and quadrature outputs needed for the carrier tracking loop. This architecture is not susceptible to pilot loss nor are any of the remaining architectures. Quadrature multipath is cancelled by a Hilbert transform process. The third type processes both the in-phase and quadrature components with complex valued coefficients. Only an in-phase output needs to be computed since the derotator precedes the forward section. Type III cancels onbaud quadrature multipath by simple phase rotation but has decreased phase noise tracking performance due to the long delay between the derotator and the phase detector. Types IV and V contain the best of II and III with regard to the forward equalizer but with an increased cost in complexity. Type V contains a passband forward equalizer and a passband DFE and has the most robust acquisition properties of the types listed.

In selecting an architecture for a particular application, consideration also needs to be given to power consumption and die area allocated for the equalizer. For a given constraint in power and die area, use of the higher complexity architectures may result in reduced equalizer

span and therefore may not yield the highest overall performance. However, with the introduction of .18 and .13 micron IC processes, the higher complexity architectures will become the natural choices.

A second area in which many of the techniques developed for QAM can be applied to VSB is in the area of blind equalization. Although the ATSC system contains a periodic training sequence, its occurrence every 24 milliseconds is too infrequent to be used to track the dynamic multipath conditions found in urban and indoor sites. This requires the use of blind equalization between the training interval. Blind equalization itself consists of two types: decision directed which is used for tracking, and cost function based which is used for acquisition where a cost function utilizes the known statistics of the transmitted source sequence. The most widely known blind technique for acquisition of a PAM signal is Sato's Algorithm [4] which utilizes a 2^{nd} order cost function. Sato's algorithm, although it has a correspondingly lower excess mean square error than a third order function, suffers from many local minima during the convergence process. In contrast, blind acquisition of a QAM signal is a well-studied problem in which many solutions have been proposed. The best known of these techniques is the constant modulus algorithm (CMA), first proposed by Godard [5]. The most useful implementation of the CMA algorithm is a third order cost function, which unlike the Sato algorithm, does not suffer from nearly as many local minima, although at the cost of a higher excess mean square error (MSE). The CMA algorithm can be modified for VSB operation by applying a similar 3 order cost function in one dimension only [6]. Initialization of the DFE can be achieved by IIR filtering techniques similar to those used by Strolle and Jaffe [7].

Finally, decision directed carrier tracking has been well developed for QAM signaling as outlined by Lee and Messerschimdt [8] and extended to VSB [7].

Results

Table 2 lists performance data for the NXT2000, an 8-VSB receiver IC which utilizes the advanced techniques outlined in this paper. Incidentally, the IC also receives the ITU J83B 64/256 QAM signal carried on North American cable systems utilizing dual mode (QAM/VSB) demodulation, synchronization, equalization and FEC processing cores.

Table 2

Impairment	Performance
AWGN	15.1 dB CNR
NTSC Co-channel	-1.0 dB D/U
Ensemble A-G With Noise	16.2-16.6 dB CNR
Strongest Static Echo	0-0.5 dB < 0.1 usec 1.5 dB at 1 usec 2.5 dB at 15 usec 3.0 dB at 32 usec 5.0 dB at 44 usec
Single Dynamic Echo	3.0 dB at 0.1 usec (5 Hz) 3.5 dB at 1.0 usec (5 Hz) 4.0 dB at 15.0 usec (2 Hz)

Conclusion

The inadequate performance of first generation receivers can be largely attributed to the fact that they relied heavily upon techniques outlined in the ATSC reference system. These receivers, although acceptable for canceling the multipath ensembles which were typically used in the early testing, do not perform well in the presense of dynamic multipath found in urban and indoor environments. Through the use of complex signal processing (vs. real only) and blind equalization techniques derived from QAM signaling, improvements in 8-VSB receivers will continue to be made, making the reception of the ATSC DTV signals a feasible goal in urban and indoor environments.

References

[1] Mueller and Muller, "Timing Recovery in Digital Synchronous Data Receivers", IEEE Trans. On Communications, pp. 516-531, May 1976

[2] D.L. Franks, "Envelop-Derived Timing Recovery in QAM and SQAM Systems", IEEE

Trans. On Communications, pp. 1327-1331, Nov. 1975.

[3] Guide to the Use of the ATSC Digital Television Standard, ATSC, Oct. 1995

[4] Y. Sato, "A Method of Self-Recovering Equalization for Multilevel Amplitude-Modulation Systems," IEEE Trans. On Communications, pp. 679-682, Jun. 1975.

[5] D. N. Godard, "Self-recovering Equalization and Carrier Tracking in Two-dimensional Data Communication Systems," IEEE Trans. On Communications, vol. 28, no. 11, pp. 1867-1875, Oct. 1980.

[6] T.J. Endres, S.N. Hulyalkar, C.H. Strolle and T.A. Schaffer, "A Decision-Directed Constant Modulus Algorithm for Higher-Order Source Constellations", to be presented at ICASSP 2000, Istanbul, Turkey

[7] C.H. Strolle and S. T. Jaffe, Unites States Patent No. 5,799,037, August 25,1998

[8] E.A. Lee and D.G..Messerschmitt, Digital Communication, Kluwer Academic Publishers: Boston, Ma., 1988

E

spawc '99

1999 2nd IEEE Workshop on

Signal Processing Advances in Wireless Communications

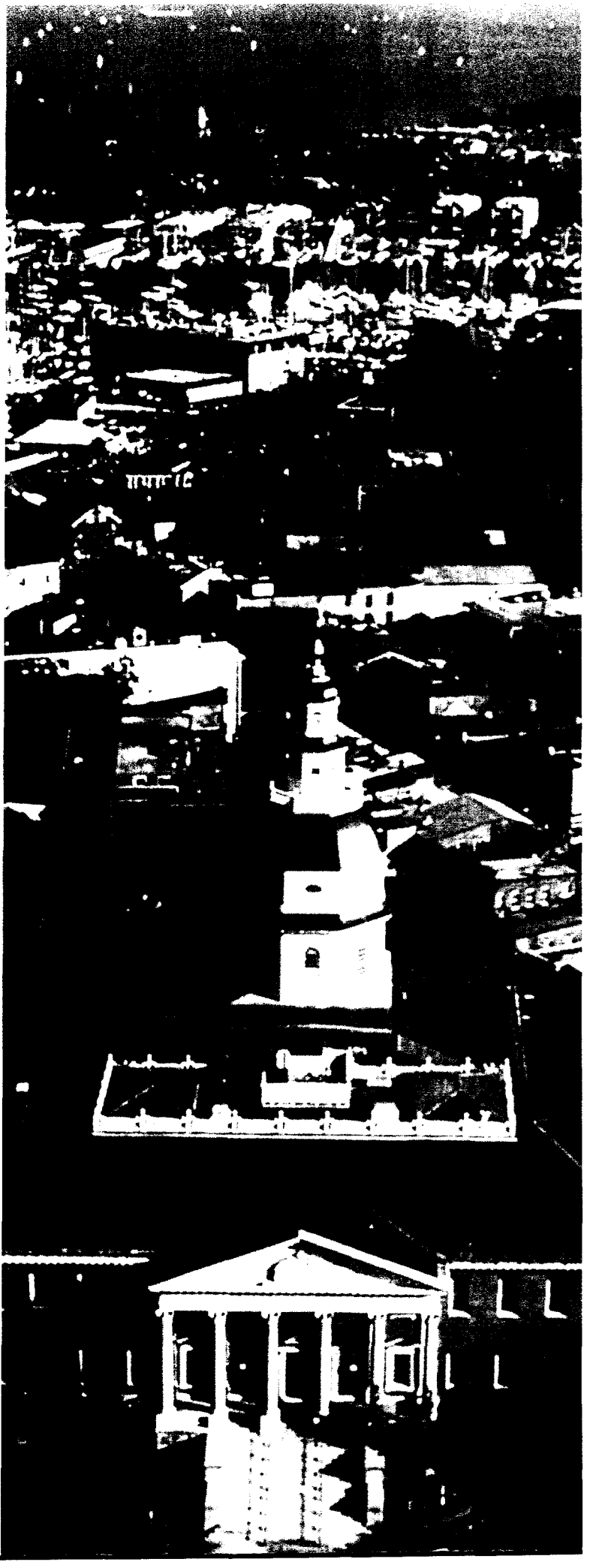

May 9-12, 1999 - Annapolis, MD, USA

CARRIER INDEPENDENT BLIND INITIALIZATION OF A DFE

T. J. Endres *C. H. Strolle* *S. N. Hulyalkar* *T. A. Schaffer* *A. Shah* *M. Gittings* *C. Hollowell*
A. Bhaskaran *J. Roletter* *B. Paratore*

Sarnoff Digital Communications, Inc.
Suite 100, 6 Penns Trail
Newtown, PA 18940 USA

ABSTRACT

This paper is concerned with the blind initialization of a decision feedback equalizer (DFE) in a practical setting. We present a DFE architecture with forward and feedback filters which operate in the passband so that equalization can be done completely independent of carrier phase. The Constant Modulus Algorithm (CMA) error term is used to update the forward and feedback equalizer parameters of a linear Infinite Impulse Response (IIR) equalizer structure in order to acquire an equalizer parameterization which is in the neighborhood of the optimum DFE setting. Methods for coarse tuning of a decision directed (DD) carrier loop during acquisition are also described. Laboratory experiments with test silicon demonstrate the similarity in equalizer parameter settings between CMA in a linear IIR structure with those of the DD least mean squares algorithm (DD-LMS) in a linear IIR structure and in a non-linear DFE structure.

1. INTRODUCTION

Digital transmission of information generally involves the modulation of pulses onto an RF carrier's amplitude and/or phase, for example, as in QAM signals. Most propagation mediums introduce distortions of the RF carrier in amplitude and phase, including inter-symbol interference (ISI) in which weighted contributions of other symbols are added to the current received symbol [2]. An equalizer is used at the receiver to mitigate this signal corruption, and it is not uncommon for the equalizer area to consume half of the total chip area. Since the specifics of the channel distortion are generally unknown at the receiver, demodulation uses adaptive methods to adjust equalizer parameters to restore signal quality to a performance level which is deemed acceptable by any subsequent error correction decoding. Equalizer parameter adjustment sometimes relies on the periodic transmission of a training or pilot sequence, and is referred to as trained equalization. Alternatively (and often desirably,) equalization algorithms are designed which do not require an explicit replica of the transmitted sequence, and are thus referred to as blind equalization algorithms.

Austin [1] was perhaps the first to propose a Decision Feedback Equalizer (DFE) in which hard decisions (or best quantized guesses of current symbol values) are filtered and fed back in order to additively cancel ISI. It is generally believed that a DFE offers better performance than that of a linear equalizer, especially for ISI-limited channels [13]. Typically, the DFE parameters are adjusted blindly using the Least Mean Squares (LMS) algorithm [17] by replacing the training symbols with hard decisions, and is therefore referred to as Decision Directed LMS (DD-LMS). Unfortunately, DD-LMS updating a DFE is usually impractical from a cold start initialization for high order constellations since high decision error rates result in error propagation and prevent algorithm convergence for most realistic channel conditions. The problem of blind DFE initialization is therefore of greatest practical concern.

The Constant Modulus Algorithm (CMA) was originally proposed by Godard [7] for QAM signals and developed independently by Treichler and Agee [15] for constant envelope FM signals. Godard's original intention was to develop an algorithm which was insensitive to carrier synchronization in order to decouple equalization and carrier tracking, so that carrier tracking could be done in a DD mode. Both [7] and [15] derived CMA for parameter adaptation of a Finite Impulse Response (FIR) filter. (We will apply the CMA update term derived in [7] and [15] to parameter adaptation of an IIR filter.)

A classical method for blind DFE initialization uses CMA to update the parameters of a linear transversal filter. Once this FIR filter has sufficiently removed enough distortion, DD carrier tracking is enabled and CMA is transferred to DD-LMS so that a baseband DFE can be used. (See [16] for an excellent discussion of this approach.) This method is quite effective, though the FIR equalizer length required can be computationally prohibitive and convergence is not guaranteed.

Another method of blind DFE initialization uses CMA to update the forward and feedback parameters of a classical non-linear DFE architecture (see [13] or [4]). This method can be sensitive to carrier frequency offset and robustness concerns with certain channel models is addressed in [3].

Our work uses CMA to blindly adjust the passband forward and feedback parameters of a linear IIR equalizer structure independent of carrier frequency or phase. During this acquisition stage, the carrier loop is coarse-tuned in order for a seamless transfer to a DD mode of operation. The equalizer parameterization acquired by CMA can then be used to start adaptation of the passband forward and feedback filters using DD-LMS in a either a linear IIR or non-linear DFE architecture. The methods discussed here are also described in U. S. Patent number 5,799,037 (reference [12]).

2. PROPOSED BLIND DFE INITIALIZATION

We are concerned with the blind initialization of DFE parameters from a cold start. To this end, we will use the equalizer architecture described in Figure 1. The equalizer receives samples which are correctly timed with the transmitter data clock, but in general are not at DC and are

0-7803-5599-7/99/$10.00©1999 IEEE

therefore spinning in the complex plane. The adaptive filters, $A(z)$ and $B(z)$, are therefore said to operate in the passband. Passband implementation offers superior acquisition for heavily impaired channels by completely decoupling carrier acquisition from equalizer convergence. See [10] for a detailed description and motivation of passband equalization strategies.

We break the adaptation process into three stages, called *acquisition*, *transfer*, and *tracking*. For each of these stages, we will relate equalizer parameter adaptation and carrier tracking to Figure 1.

Stage 1 (*acquisition*):
Path 1 is selected in Figure 1 so that a linear, IIR structure is used. Note that though $B(z)$ is a FIR filter, it is embedded in a feedback loop which results in an overall infinite impulse response. The equalizer parameters are adapted from a cold-start initialization (for example, $A(z) = [\,0\;0\;...\;0\;1\;0\;...\;0]^T$ and $B(z) = [\,0\;0\;...\;0]^T$) using the CMA update term, i.e,.

$$A_{k+1} = A_k + \mu z_k(\gamma - |z_k|^2)\mathbf{r_k^*} \quad (1)$$

$$B_{k+1} = B_k + \mu z_k(\gamma - |z_k|^2)\mathbf{z_k^*} \quad (2)$$

where μ is a small, positive, stepsize, $\mathbf{r(k)} = [r_k\; r_{k-1}\; ...\; r_{k-M+1}]^T$ is a regressor vector of inputs to length-M $A(z)$, and $\mathbf{z_k} = [z_{k-1}\; z_{k-2}\; ...\; z_{k-N}]^T$ is a regressor vector of inputs to length-N $B(z)$. Observe that $\mathbf{z_k}$ is composed of equalizer output samples.

While using CMA to update the equalizer parameters, the carrier tracking loop is operated in a coarse fashion by treating the signal as if it is from a QPSK constellation. That is, the carrier tracking loop attempts to force the sample's phase to a multiple of $\pi/4$. We have found that even for dense QAM constellations with severe multipath, this coarse tuning of the carrier loop allows for a smooth transition to a DD mode of operation.

The *acquisition* stage is switched to the *transfer* stage after a prescribed number of symbol iterations or until a performance measure falls below a prescribed threshold. Observe that the carrier tracking loop is completely decoupled from the equalizer during the *acquisition* stage.

Stage 2 (*transfer*):
Path 1 is selected in Figure 1 so that a linear, IIR structure is used. Parameter adaptation is still blind, though the CMA update term from the *acquisition* stage is replaced by the DD Least Mean Squares (DD-LMS) update term. The adaptive filters are adjusted according to the rule

$$A_{k+1} = A_k + \mu(\hat{z}_k - z_k)\mathbf{r_k^*} \quad (3)$$

$$B_{k+1} = B_k + \mu(\hat{z}_k - z_k)\mathbf{z_k^*} \quad (4)$$

The carrier tracking loop during the *tracking* stage is switched from its coarse tuning in the *acquisition* stage to a standard decision directed operation mode. The soft decision ($z_k e^{-j\theta(k)}$) and hard decision ($Q[z_k e^{-j\theta(k)}]$) are input to the the carrier tracking loop. ($Q[\cdot]$ here denotes quantization from the decision device.) To the extent that there exists a phase difference, an error signal is generated to adjust the phase estimate ($\theta(k)$). See [11] for a detailed description of DD carrier tracking strategies.

The *transfer* stage is switched to the *tracking* stage after a prescribed number of symbol iterations or until a performance measure falls below a prescribed threshold.

Table 1. Description of multipath used in laboratory experiment

Multipath Delay (μsec)	Loss (dB)
-0.4	10
0	0
+0.9	7
+1.15	15
+1.85	19

Stage 3 (*tracking*):
Path 2 is selected in Figure 1 so that a non-linear, DFE structure is used. The path 2 branch contains a de-rotator and re-rotator in order to accomplish the slicing (decision device) on a baseband, rather than passband, sample. For example, the passband equalizer output sample, z, is multiplied by the estimate of the carrier offset ($e^{-j\theta(k)}$) to form the baseband soft decision (or input to the decision device). The output of the decision device (or hard decision) is a baseband sample and is re-rotated by multiplication with $e^{+j\theta(k)}$ to form the sample $\hat{z}$. Hence, we refer to the $\hat{z}$ samples as passband hard decisions.

Equalizer parameter adaptation is done using the DD-LMS error term, and the carrier loop is run in a DD mode, as was done in the *transfer* stage, so that the update of $A(z)$ remains unchanged from the *transfer* stage. The regressor vector of input samples to $B(z)$, however, is comprised of passband hard decisions, so that $B(z)$ is adjusted according to the rule

$$B_{k+1} = B_k + \mu(\hat{z}_k - z_k)\hat{\mathbf{z}}_\mathbf{k}^* \quad (5)$$

where $\hat{\mathbf{z}}_\mathbf{k} = [\hat{z}_{k-1}\; \hat{z}_{k-2}\; ...\; \hat{z}_{k-N}]^T$ is the regressor vector of passband hard decisions which are input to $B(z)$.

3. EMPIRICAL RESULTS

We have developed silicon which utilizes the equalizer architecture described in Figure 1. The SDC1000 is a high speed receiver which contains an internal 10-bit A/D converter and can be configured for 64- or 256-QAM demodulation. The 32-tap equalizer can be programmed to allocate equalizer parameters between $A(z)$ and $B(z)$. Though the SDC1000 contains forward error correction (FEC) which is ITU-J.83B compliant, we will study the equalizer parameters and equalizer output prior to error correction.

Laboratory testing of the SDC1000 used a TAS Model 4500 multipath generator which introduces multipath at an RF frequency of approximately 500 MHz. The received signal is downconverted to an IF frequency of 44 MHz using a consumer grade, real-world tuner. The multipath introduced in this experiment is summarized in Table 1.

The SDC1000 is configured so that the length of $A(z)$ is $M = 12$ and the length of $B(z)$ is $N = 20$. The symbol rate is approximately 5.36 MHz with 256-QAM signaling. The equalized 256-QAM output after stage 3 is shown in Figure 2.

Figures 3, 4, and 5 show the equalizer parameter vector upon convergence for stage 1 (*acquisition*), stage 2 (*transfer*), and stage 3 (*tracking*), respectively. In each of these figures, the first plot is the I component of the parameter vector, the second plot is the Q component of the parameter vector, and the third plot is the magnitude of the parameter vector. In each of these figures, the first 12 parameters

correspond to $A(z)$, while the remaining 20 parameters correspond to $B(z)$.

Observe that the magnitudes of the parameter vectors for the three stages are nearly identical. The I and Q components of the three stages, however, suggest that the parameter vectors for the three stages are rotated versions of one another. The architecture in Figure 1 allows free rotation of the parameter vector, independent of carrier phase.

These results suggest that there exist minima settings for CMA in a linear IIR feedback structure which are in a close neighborhood to minima settings for DD-LMS in either a linear IIR feedback structure or in a non-linear DFE structure.

4. CONCLUDING REMARKS

The intent of this paper is to describe to the reader an architecture and algorithms that can be reliably used for the blind initialization of a DFE without the need for precise carrier lock. We believe this problem to be of utmost practical concern. Though we have borrowed the CMA update term from [7] and [15] and applied it to an IIR equalizer structure, we have not shown that such a parameter update minimizes the CM cost function. Recognize that our methods include simplifications that ease implementation. Namely, the true CM-minimizing update error term is shown in [5] to include regressor filtering by the time-varying equalizer parameters. Our methods neglect this regressor filtering for implementation ease as was done in [6] which used an LMS-style error term. Johnson and Larimore [9] show the sensitivity of the algorithm in [6] by illustrating the multi-modal squared error cost surface with an example which is undermodeled (i.e., there are too few equalizer parameters to exactly model the channel). Reference [14] addresses the stability concerns of the algorithm of [6] to channel models which are not strictly positive real (SPR). [1]

Though we have introduced stage 2 (*transfer*) into our blind initialization strategy, which uses DD-LMS in a linear IIR structure, we have found that stage 2 can be bypassed in many situations and CMA in a linear IIR structure can be transferred directly to a DFE structure using DD-LMS. Our results provide evidence that CMA in a linear IIR structure admits minima settings which are in close proximity to (i) the minima settings of DD-LMS used in a linear IIR feedback structure, and (ii) the minima settings of DD-LMS used in a non-linear DFE structure.

REFERENCES

[1] M. Austin, "Decision feedback equalization for digital communication over dispersive channels," *MIT Research Laboratory of Electronics Technical Report 461*, Cambridge, MA, August 1967.

[2] P. A. Bello, "Characterization of randomly time-invariant linear channels," *IEEE Transactions on Communication Systems*, vol. CS-11, pp.360-393, Dec. 1963.

[3] R. A. Casas, "Blind adaptive decision feedback equalization: a class of *bad* channels," *M. S. Dissertation*, Cornell University, Ithaca, NY, May 1996.

[4] R. A. Casas, Z. Ding, R. A. Kennedy, C. R. Johnson, Jr., R. Malamut, "Blind adaptation of decision feedback equalizers based on the constant modulus algorithm," *Asilomar Conference on Signals, Systems and Computers*, Pacific Grove, CA, pp. 698-702, Oct.-Nov. 1995.

[5] R. A. Casas, C. R. Johnson, Jr., J. Harp, S. P. Caffee, "On initialization strategies for blind adaptive DFEs," *Proceedings of the Wireless Communications and Networking Conference (to appear)*, New Orleans, LA, Sept. 1999.

[6] P. L. Feintuch, "An adaptive recursive LMS filter," *Proccedings of the IEEE*, vol. 64, no. 11, pp. 1622-24, Nov. 1976.

[7] D. N. Godard, "Self-Recovering Equalization and Carrier Tracking in Two-Dimensional Data Communication Systems," *IEEE Trans. on Communications*, vol. 28, no. 11, pp. 1867-1875, Oct. 1980.

[8] C. R. Johnson, Jr., P. Schniter, T. J. Endres, J. D. Behm, D. R. Brown, R. A. Casas, "Blind Equalization Using the Constant Modulus Criterion: A Review," *Proccedings of the IEEE*, vol. 86, no. 10, pp. 1927-1950, Oct. 1998.

[9] C. R. Johnson, Jr., M. G. Larimore, "Comments on and additions to 'An adaptive recursive LMS filter'," *Proccedings of the IEEE*, vol. 65, no. 9, pp. 1399-1402, Sept. 1977.

[10] E. A. Lee, D. G. Messerschmitt, *Digital Communications*, Boston, MA: Kluwer Academic Publishers, 1988.

[11] H. Meyr, M. Moeneclaey, S. A. Fechtel, *Digital Communication Receivers*, New York, NY: John Wiley and Sons, 1998.

[12] C. H. Strolle, S. T. Jaffe, "Receiver capable of demodulating multiple digital modulation formats," *United States Patent*, Patent no. 5,799,037, Aug. 25, 1998.

[13] L. Tong, D. Liu, H. Zeng, "On blind decision feedback equalization," *Asilomar Conference on Signals, Systems and Computers*, Pacific Grove, CA, pp. 305-309, Nov. 1996.

[14] J. R. Treichler, C. R. Johnson, Jr., M. G. Larimore, *Theory and Design of Adaptive Filters*, New York, NY: John Wiley and Sons, 1987.

[15] J.R. Treichler and B.G. Agee, "A New Approach to Multipath Correction of Constant Modulus Signals," *IEEE Trans. on Acoustics, Speech, and Signal Proc.*, vol. ASSP-31, no. 2, pp. 459-72, April 1983.

[16] J. R. Treichler, M. G. Larimore, J. C. Harp, "Practical blind demodulators for high-order QAM signals," *Proccedings of the IEEE*, vol. 86, no. 10, pp. 1907-1926, Oct. 1998.

[17] B. Widrow, J. McCool, M. Ball, "The complex LMS algorithm," *Proccedings of the IEEE*, vol. 63, no. 4, pp. 719-720, April 1975.

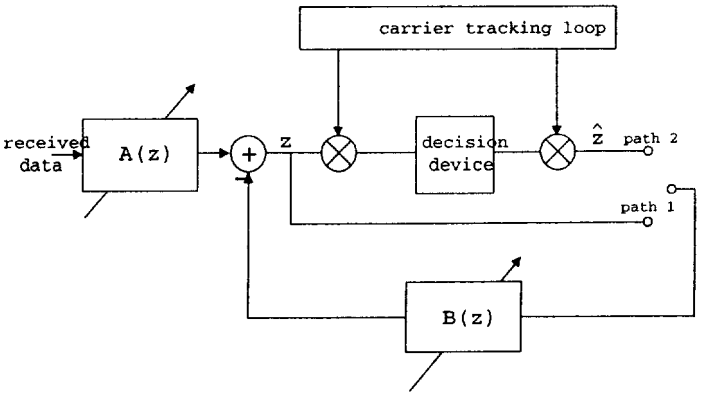

Figure 1. Proposed architecture for the blind, carrier-independent initialization of a DFE

[1] Strictly positive real (SPR) means that the real part of the channel's frequency response is strictly positive. Hence, the phase of the channel's transfer function is constrained to be within (-90,+90) degrees. See [14].

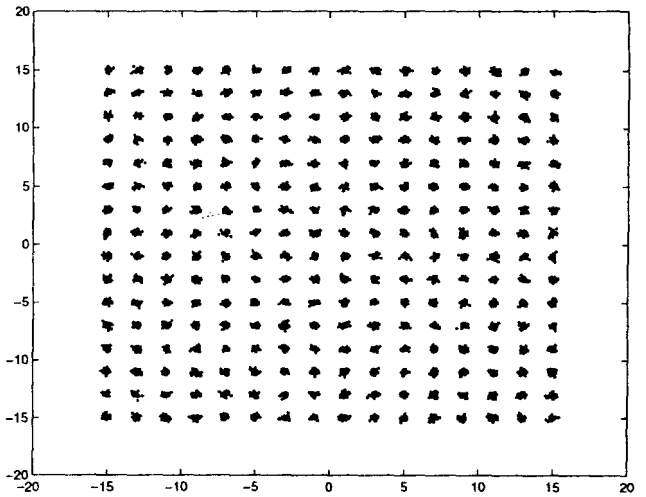

Figure 2. 256-QAM constellation of test silicon using the equalizer architecture in Figure 1. The equalizer and carrier tracking loop have converged under the non-linear DFE *tracking* mode.

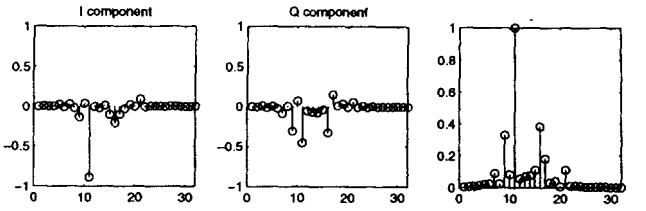

Figure 4. Equalizer parameter vector at end of Stage 2 (DD-LMS,IIR with DD carrier). First plot is I component of equalizer parameters; Second plot is Q component of equalizer parameters; Third plot is magnitude of equalizer parameters.

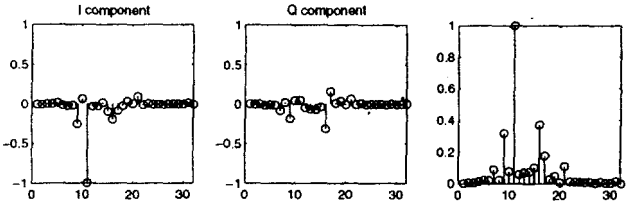

Figure 3. Equalizer parameter vector at end of Stage 1 (CMA,IIR with rough carrier). First plot is I component of equalizer parameters; Second plot is Q component of equalizer parameters; Third plot is magnitude of equalizer parameters.

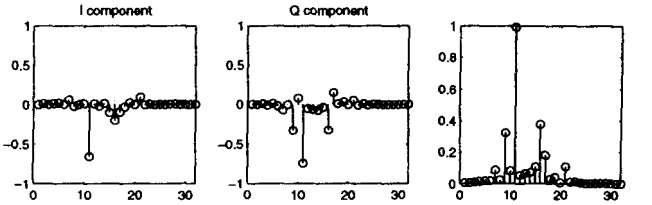

Figure 5. Equalizer parameter vector at end of Stage 3 (DD-LMS,DFE with DD carrier). First plot is I component of equalizer parameters; Second plot is Q component of equalizer parameters; Third plot is magnitude of equalizer parameters.

On Sparse Equalization Using Mean-Square-Error and Constant Modulus Criteria

T. J. Endres, R. A. Casas, S. N. Hulyalkar, and C. H. Strolle
NxtWave Communications
One Summit Square
Langhorne, PA 19047
e-mail: {endres,raul,samirh,cstrolle,}@nxtwavecomm.com

Abstract — **This paper considers the utility of implementing sparse equalizers with the Mean Square Error (MSE) and Constant Modulus (CM) criteria. A sparse equalizer does not constrain the equalizer parameters to be adjacent or contiguous in the tapped delay line, while vacant positions in the tapped delay line are constrained to be zero-valued. We motivate the use for sparse equalizers, and show that both the MSE and CM cost functions admit sparse minima settings in near proximity to the full-length Wiener settings.**

I. Introduction

Modern digital receivers use some type of adaptive equalization or channel correction in order to compensate for distortions introduced during transmission. These functions are adaptive since a precise description of the channel characteristics is not available at the receiver. Because channel conditions tend to vary over time, adaptation is not halted upon convergence. As a result of a non-vanishing error term, the equalizer parameters rattle around the (local) minimum setting. This stochastic jitter (often called misadjustment) induces an increase in the overall MSE seen at the output of the demodulator. The penalty in terms of excess MSE (EMSE) induced by stochastic jitter is known to be proportional to the number of equalizer parameters that are updated and the value of non-vanishing stepsize. Hence, more equalizer parameters induce a larger EMSE penalty.

On the other hand, the depth of the (local) minimum setting, which represents the MSE achievable decreases as the number of equalizer parameters is increased, so that a lower MMSE floor is achieved by a longer equalizer than a shorter one. For high data-rate signaling through dispersive channel conditions, the length of the equalizer must be chosen to compensate for the delay spread of the channel. This equalizer length can be significant. For example, in terrestrial broadcast of high definition television (HDTV) signals, the data rate is approximately 10.76 Megabaud, and the channel delay spread typically documented for UHF television is about 44 usec. Hence, an equalizer length of about 500 is desirable from a MMSE viewpoint. The designer is therefore faced with a classical tradeoff–the equalizer length should be chosen long enough for sufficient MSE performance, but not so long that EMSE dominates. For example, see [8] which discusses these conflicting requirements. The EMSE penalty can be significant to the extent that the required reduction in stepsize can cripple equalizer tracking capabilities.

In most studies of equalizer length, it is implicitly assumed that the equalizer parameters are adjacent, or contiguous, in the tapped-delay-line. We wish to remove this constraint by allowing for a longer tapped-delay-line, where parameters corresponding to unused positions are zero-valued. Such a construction is called a *sparse equalizer* and is desirable (i) from an implementation point of view, and (ii) from a MSE point of view. First, the number of multipliers needed in the filtering and adaptation processes is reduced compared to the full equalizer length. Since multipliers are costly real-estate and the adaptive equalizer footprint is typically over half of the total chip area, the sparse construction can significantly ease implementation and reduce power consumption. Second, since the number of equalizer parameters seeing a non-zero update error term is reduced compared to the full equalizer length, the EMSE (or stochastic jitter) is reduced. This reduction allows the use of a higher stepsize compared to a full-length equalizer, so that tracking capabilities of the sparse equalizer are improved.

The objective of this paper is to study the feasibility of a sparse equalizer minimizing the Constant Modulus (CM) and MSE criteria. The Constant Modulus Algorithm (CMA) is commonly used as a blind, acquisition aid in conjunction with the Least Mean Squares (LMS) algorithm in a decision-directed mode for tracking. We therefore study the effect of discarding small equalizer parameters in the optimum Wiener setting by forcing these parameters to a zero value. We show the close proximity of sparse CM and MSE minima settings to full-length Wiener settings and the sensitivity of MSE performance on system delay. Next, Section II describes the system model and derives sparse Wiener settings. Section III describes the relationship between sparse CM and MSE settings for QAM signaling. Section IV presents performance results using computer simulations and laboratory experiments, and Section V provides concluding remarks.

II. System Model and Wiener Settings

The communication system considered is a baseband, linear model which samples the received signal at a fraction $(1/L)$ of the baud interval, T. We further assume that synchronization is accomplished independently of equalization; the channel is therefore modeled with a time-invariant finite impulse response (FIR) whose coefficients are contained in a length-Q T/L-spaced vector $\mathbf{c} = (c_0\ c_1\ \ldots\ c_{Q-1})^T$. Similarly, the equalizer is described by a length-N T/L-spaced vector of coefficients $\mathbf{f} = (f_0\ f_1\ \ldots\ f_{N-1})^T$.

The T-spaced combined channel-equalizer, $\mathbf{h}(= \mathbf{Cf},)$ is a length-P vector which in the absence of noise maps the baud-spaced source sequence, s_k, to the baud-spaced equalizer output, y_k, via the (block) Toeplitz channel convolution matrix,

for example,

$$\underbrace{\begin{pmatrix} h_0 \\ h_1 \\ \vdots \\ h_{P-1} \end{pmatrix}}_{\mathbf{h}} = \underbrace{\begin{pmatrix} c_1 & c_0 & & & \\ c_3 & c_2 & & & \\ \vdots & \vdots & \ddots & c_1 & c_0 \\ c_{Q-1} & c_{Q-2} & \ddots & c_3 & c_0 \\ & & \ddots & \vdots & \vdots \\ & & & c_{Q-1} & c_{Q-2} \end{pmatrix}}_{\mathbf{C}} \underbrace{\begin{pmatrix} f_0 \\ f_1 \\ \vdots \\ f_{N-1} \end{pmatrix}}_{\mathbf{f}} \quad (1)$$

where $L = 2$ is chosen for convenience. See [5] and references therein for more details of this system model.

A. MMSE Equalizer Coefficients

We seek a description of the equalizer coefficients which minimize the MSE cost using M ($M \leq N$) equalizer coefficients which are not constrained to be contiguous (or adjacent) in the length-N equalizer tapped delay line. The remaining $N - M$ equalizer coefficients are constrained to zero. These settings are referred to as the *sparse Wiener settings*. See [10] for a related approach to find these settings. Also note that for a fixed number of equalizer parameters, M, choosing $N = M$ (forcing all equalizer parameters to be contiguous) is a subset of $N \geq M$ and is therefore sub-optimal.

We first review "full-length" Wiener settings, i.e., $M = N$. When the source symbols are temporally independent and equiprobable at each baud instance (i.e., white and i.i.d.) and the additive noise is white and gaussian, the MSE cost can be expressed as (see [6])

$$J_{MSE} = \sigma_s^2 \left(\mathbf{e}_\delta - \mathbf{C}\mathbf{f}\right)^H \left(\mathbf{e}_\delta - \mathbf{C}\mathbf{f}\right) + \sigma_n^2 \mathbf{f}^H \mathbf{f} \quad (2)$$

where $\mathbf{e}_\delta$ is the desired response for the combined channel-equalizer (a pure delay) and therefore contains a single non-zero coefficient of unit value in the δ^{th} index, σ_s^2 is the variance of the zero-mean source sequence, and σ_n^2 is the variance of the zero-mean additive noise process. The Wiener settings minimize (2) and can be found by a variety of methods (pseudo-inverse, completing the square, calculus over complex vectors, etc.) and are described by (see [6])

$$\mathbf{f}^\dagger = \left(\mathbf{C}^H\mathbf{C} + \lambda \mathbf{I}_N\right)^{-1} \mathbf{C}^H \mathbf{e}_\delta \quad (3)$$

where $\lambda = \sigma_n^2/\sigma_s^2$. We solve for the sparse Wiener settings by manipulating the MSE cost for a sparse equalizer tapped delay line to resemble (2).

Let $\mathcal{A}$ be the set of M elements equal to the indices which are to be used in the equalizer tapped delay line. For example, $\mathcal{A} = \{0, 1, 3\}$ if (for $N = 4$ and $M = 3$,) f_0, f_1, and f_3 are to be used while f_2 is to be zeroed. Let $\mathcal{B}$ be the set $\mathcal{B} = \{0, 1, \ldots, M-1\}$. Define $\mathbf{f}_s$ as the length-N equalizer vector with zeros for coefficients with indices not in $\mathcal{A}$. (For the above example, $\mathbf{f}_s = (\ f_0\ f_1\ 0\ f_3\ )^T$.) Similarly, define $\hat{\mathbf{f}}_s$ as the length-M vector which contains the non-zero elements of $\mathbf{f}_s$ in the same order that they appeared in $\mathbf{f}_s$. (For the example, $\hat{\mathbf{f}}_s = (\ f_0\ f_1\ f_3\ )^T$.) Define the matrix $\mathbf{P}$ as the $N \times M$ matrix with elements (row i, column j) $\mathbf{P}_{i,j} = 1$ if $(i,j) \in \mathcal{A}\mathcal{X}\mathcal{B}$ and 0 otherwise, where $\mathcal{X}$ denotes cartesian product. For the above example,

$$\mathbf{P} = \begin{pmatrix} 1 & 0 & 0 \\ 0 & 1 & 0 \\ 0 & 0 & 0 \\ 0 & 0 & 1 \end{pmatrix} \quad (4)$$

Observe that with these definitions, $\mathbf{f}_s = \mathbf{P}\hat{\mathbf{f}}_s$ and that $\mathbf{P}^H\mathbf{P} = \mathbf{I}_M$. The MSE for a sparse equalizer can therefore be written as

$$J_{MSE|sparse} = \sigma_s^2 \left(\mathbf{e}_\delta - \hat{\mathbf{C}}\hat{\mathbf{f}}_s\right)^H \left(\mathbf{e}_\delta - \hat{\mathbf{C}}\hat{\mathbf{f}}_s\right) + \sigma_n^2 \hat{\mathbf{f}}_s^H \hat{\mathbf{f}}_s \quad (5)$$

where $\hat{\mathbf{C}} = \mathbf{C}\mathbf{P}$. Equating (5) with (2), the sparse Wiener coefficients follow immediately as

$$\hat{\mathbf{f}}_s^\dagger = \left(\hat{\mathbf{C}}^H\hat{\mathbf{C}} + \lambda \mathbf{I}_M\right)^{-1} \hat{\mathbf{C}}^H \mathbf{e}_\delta \quad (6)$$

Note that $\mathbf{f}_s^\dagger = \mathbf{P}\hat{\mathbf{f}}_s^\dagger$ is the optimum length-N vector with $N - M$ coefficients not in $\mathcal{A}$ constrained to zero.

As Treichler and Larimore [10] point out, since the effect of multiplication on the left (right) by $\mathbf{P}$ is to remove rows (columns) of a given matrix, the eigenstructure of $\hat{\mathbf{C}}^H\hat{\mathbf{C}}$ can be different than $\mathbf{C}^H\mathbf{C}$. Hence, for adaptive algorithms whose stability and convergence rate depend on the maximum and minimum eigenvalues of the data covariance matrix (such as LMS,) it is not inconceivable that a well-designed sparse equalizer can achieve better dynamic convergent behavior and better static performance at equilibrium than a standard equalizer.

As an example, we compare the MMSE performance of a sparse and full-length equalizer by evaluating (3) and (6) versus number of equalizer parameters. The length-300 channel model is chosen as channel 3 from the database at

http://spib.rice.edu

with 30 dB SNR. (Note that this channel is plotted in the top subplot of Figure 3.) The set $\mathcal{A}$ is chosen as the largest M coefficients in magnitude from the length-300 Wiener setting found according to (3), and the system delay, δ, is optimum. Figure 1 shows the MMSE performance versus number of active equalizer parameters. Observe that fewer sparse equalizer coefficients than full-length equalizer coefficients are needed to reach a target threshold. Also, the "knee" in the curve for the full-length equalizer at approximately $M = 55$ results from inadequacy in spanning the delay spread of the channel containing significant energy for $M < 55$. On the other hand, the sparse equalizer distributes equalizer parameters more effectively and spans the delay spread of the channel with fewer equalizer parameters. For example, fixing $M = 50$ in Figure 1, we show the magnitude of the parameters for the sparse equalizer, full-length equalizer, sparse equalizer-channel response, and full-length equalizer-channel response in Figure 2.

B. Optimum System Delay

It is well demonstrated that MSE performance can be extremely sensitive to the choice of system delay, δ. We now provide a closed-form expression for the optimum system delay of a sparse equalizer. The MSE in (2) evaluated at the sparse Wiener setting in (6) can be reduced to

$$J_{MSE}|_{\hat{\mathbf{f}}_s^\dagger} = \sigma_s^2 \mathbf{e}_\delta^H \left[\mathbf{I}_P - \hat{\mathbf{C}}(\hat{\mathbf{C}}^H\hat{\mathbf{C}} + \lambda \mathbf{I}_M)^{-1}\hat{\mathbf{C}}^H\right] \mathbf{e}_\delta \quad (7)$$

Since $\mathbf{e}_\delta$ is a pure delay, the choice of delay therefore selects the main diagonal element of the bracketed matrix in (7). With the objective being selection of δ corresponding to a minimum MSE setting, the optimum delay choice for a sparse equalizer

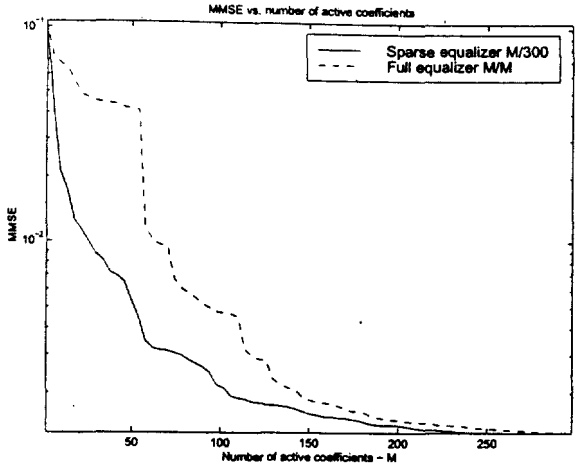

Figure 1: MMSE performance versus number of equalizer parameters for a sparse and full-length equalizer.

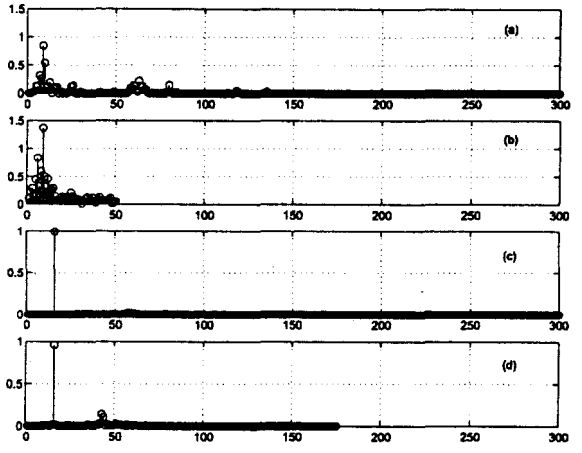

Figure 2: Magnitude of (a) sparse-equalizer parameters (M/N = 50/300), (b) full-length equalizer parameters (M/N = 50/50), (c) sparse equalizer-channel response, and (d) full-length equalizer-channel response.

corresponds to the minimum main diagonal element of this matrix, or

$$\delta^{\dagger}_{sparse} = \arg\min_{\delta} \left\{ \left[\mathbf{I}_P - \hat{\mathbf{C}}(\hat{\mathbf{C}}^H\hat{\mathbf{C}} + \lambda\mathbf{I}_M)^{-1}\hat{\mathbf{C}}^H \right]_{\delta,\delta} \right\} \quad (8)$$

To demonstrate the sensitivity of the system delay on a sparse equalizer, we evaluate the MMSE at the optimum sparse Wiener settings in (6) for all possible system delays. The $T/2$-spaced channel model is derived from empirical signals and available from the database at **http://spib.rice.edu**, designated as Channel 3. The set $\mathcal{A}$ is chosen as the positions corresponding to the largest M coefficients of the full-length Wiener setting found according to (3). Note that the channel length is 300 so we set $N = 300$. The equalizer parameters corresponding to the unused $N - M$ positions are zero-valued.

Figure 3 shows the channel impulse response magnitudes and the MSE versus system delay for $M = 32$ and $M = 64$. This figure suggests strong dependence on δ. Note that for

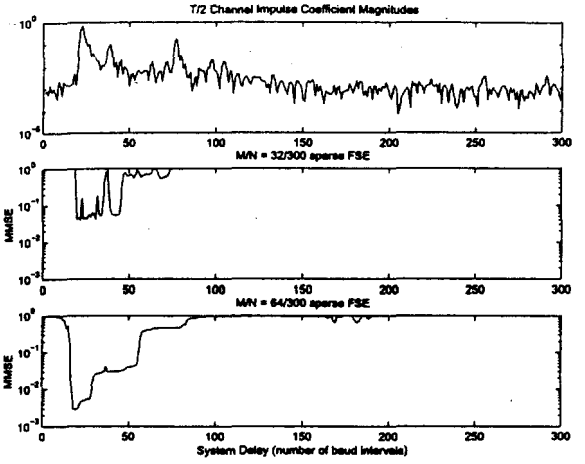

Figure 3: Channel 3 impulse response magnitudes and system delay dependence for a sparse equalizer.

$M = 32$, this dependence is evidenced as steep jumps in the sensitivity of MSE to delay. For $M = 64$, however, the system is less undermodeled and the sensitivity to delay is smoother.

III. CM and MSE Costs Using a Sparse Equalizer

We desire a description of the CM cost surface in the vicinity of a local minimum using a sparse equalizer. We will use QAM signalling and follow the approach in [1].

Let $\mathbf{f}^{\dagger}$ be a length-N Wiener setting described by (3) with $\sigma_n^2 = 0$ which achieves perfect equalization and is also equal to a CM global minimum setting [7]. This vector is described by $\mathbf{f}^{\dagger} = (\, f_0^{\dagger}\ f_1^{\dagger}\ \cdots\ f_{N-1}^{\dagger}\,)$. Let $\mathbf{f}_s$ be the length-N vector containing those M coefficients of $\mathbf{f}^{\dagger}$ with indices in the set $\mathcal{A}$ and zeros elsewhere. (For the example in §II, $\mathbf{f}_s = (\, f_0^{\dagger}\ \ f_1^{\dagger}\ \ 0\ \ f_2^{\dagger}\,)^T$.) Similarly, define $\tilde{\mathbf{f}}$ as the length-N vector with zeros corresponding to the indices in $\mathcal{A}$ and coefficients of $\mathbf{f}^{\dagger}$ elsewhere. (Continuing the example, $\tilde{\mathbf{f}} = (\, 0\ \ 0\ \ -f_3^{\dagger}\ \ 0\,)^T$.) Hence, we can express the sparse equalizer as $\mathbf{f}_s = \mathbf{f}^{\dagger} + \tilde{\mathbf{f}}$. The combined channel-equalizer for the sparse equalizer may therefore be expressed as $\mathbf{h} = \mathbf{h}_m + \mathbf{h}_s$ with $\mathbf{h}_m = \mathbf{C}\mathbf{f}^{\dagger}$ and $\mathbf{h}_s = \mathbf{C}\tilde{\mathbf{f}}$. Since $\mathbf{f}^{\dagger}$ achieves perfect equalization, there is no error in the equalized signal due to $\mathbf{h}_m$. On the other hand, $\mathbf{h}_s$ is the result of equalizer coefficients omitted in the sparse tapped delay line which causes an error in the equalized signal. Our goal is to determine the effect of $\mathbf{h}_s$ on the CM criterion for QAM signalling and describe the MSE performance.

A. QAM CM Criterion with Sparse Equalizer

The CM criterion is expressed as $J_{CM} = E\{(|y_k|^2 - \gamma)^2\}$ (see [4] or [11]) where γ is the Godard radius. For QAM signalling in the absence of noise, the CM cost can be expanded in terms of $\mathbf{h}$ and some source statistics and expressed as (see [5])

$$\begin{aligned} J_{CM|QAM} \quad (9)\\ = \ & \kappa_s(\sigma_s^2)^2 \sum_{i=0}^{P-1} |h_i|^4 + 2(\sigma_s^2)^2 \sum_{i=0}^{P-1}\sum_{l=0,l\neq i}^{P-1} |h_i|^2|h_l|^2 \\ - \ & 2(\sigma_s^2)^2\kappa_s\|\mathbf{h}\|_2^2 + (\sigma_s^2)^2\kappa_s^2 \end{aligned}$$

where $\kappa_s = \frac{E\{|s|^4\}}{E^2\{|s|^2\}}$ is the normalized source kurtosis. Observe that the CM cost at a global minima setting which achieves perfect equalization can be found by evaluating (9) with $\mathbf{h}$ as a pure delay,

$$J_{CM|QAM|global} = (\sigma_s^2)^2 (\kappa_s^2 - \kappa_s) \quad (10)$$

For a sparse equalizer, we have that $\mathbf{h} = \mathbf{h_m} + \mathbf{h_s}$, or $h_i = m_i + p_i$ where $h_i \in \mathbf{h}$, $m_i \in \mathbf{h_m}$, and $p_i \in \mathbf{h_s}$. Since $\mathbf{h_m}$ is the combined channel-equalizer response corresponding to a global minimum of the CM cost function, $m_i = e^{j\theta}$ if $i = \delta$ and 0 otherwise, where θ is an unknown phase shift due to the CM criterion's phase insensitivity.

Hence, the contributions of (9) can be written as

$$\|\mathbf{h}\|_2^2 = \sum_{i=0, i\neq\delta}^{P-1} |p_i|^2 + 1 + e^{-j\theta} p_\delta + e^{j\theta} p_\delta^* \quad (11)$$

$$\sum_{i=0}^{P-1} |h_i|^4 = \sum_{i=0}^{P-1} |p_i|^4 + 2(p_\delta^*)^2 p_\delta e^{j\theta} + 2p_\delta^2 p_\delta^* e^{-j\theta} + 4|p_\delta|^2 \quad (12)$$
$$+ (p_\delta^*)^2 e^{2j\theta} + p_\delta^2 e^{-2j\theta} + 2(p_\delta e^{-j\theta} + p_\delta^* e^{j\theta}) + 1$$

and for the double sum

$$\sum_{i=0}^{P-1} \sum_{l=0, l\neq i}^{P-1} |h_i|^2 |h_l|^2 = \sum_{i=0, i\neq\delta}^{P-1} |p_i|^2 \left(2 + 2p_\delta^* e^{j\theta} + 2p_\delta e^{-j\theta}\right) + \sum_{i=0}^{P-1} \sum_{l=0, l\neq i}^{P-1} |p_i|^2 |p_l|^2 \quad (13)$$

Collecting terms (11), (12), and (13), substituting into (9) and subtracting (10), we bound (by optimality) the change in the CM cost from a perfect setting due to a sparse tapped delay line,

$$\begin{aligned} &\Delta J_{CM|QAM|sparse} \quad (14)\\ &= \kappa_s(\sigma_s^2)^2 \left(p_\delta^2 e^{-2j\theta} + (p_\delta^*)^2 e^{2j\theta} + 4|p_\delta|^2\right)\\ &+ \sum_{i=0, i\neq\delta}^{P-1} |p_i|^2 \left((\sigma_s^2)^2 (4 - 2\kappa_s)\right)\\ &+ 2\kappa_s(\sigma_s^2)^2 \left(p_\delta^2 p_\delta^* e^{-j\theta} + (p_\delta^*)^2 p_\delta e^{j\theta}\right)\\ &+ 4(\sigma_s^2)^2 \sum_{i=0, i\neq\delta}^{P-1} |p_i|^2 \left(p_\delta^* e^{j\theta} + p_\delta e^{-j\theta}\right)\\ &+ \kappa_s(\sigma_s^2)^2 \sum_{i=0}^{P-1} |p_i|^4 + 2(\sigma_s^2)^2 \sum_{i=0}^{P-1} \sum_{l=0, l\neq i}^{P-1} |p_i|^2 |p_l|^2 \end{aligned}$$

Observe that the terms in (14) are grouped according to powers of the p_i. When the coefficients which are omitted in the sparse tapped delay line (i.e., those non-zero elements of $\tilde{\mathbf{f}}$) are small, the p_i are also small, so that (14), which is made up of quadratic, cubic, and quartic contributions of the p_i, is itself small. In this case the local minima of the sparse CM cost function stay in close proximity to the full-length settings.

B. Relation to MSE

The MSE cost function can be expressed in terms of h_i as

$$J_{MSE} = \sigma_s^2 \left(\sum_{i=0}^{P-1} |h_i|^2 - h_\delta^* - h_\delta + 1\right) \quad (15)$$

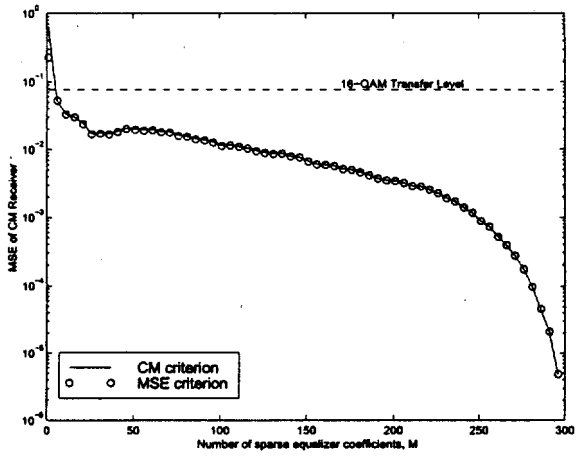

Figure 4: MSE performance for sparse CM receiver (solid) and for MSE receiver (circles), both versus the number of equalizer parameters, M.

Letting $h_i = m_i + p_i$ implies that

$$\begin{aligned} &J_{MSE|sparse} \quad (16)\\ &= \sigma_s^2[2 - 2\cos\theta + p_\delta(e^{-j\theta} - 1) + p_\delta^*(e^{j\theta} - 1) + \sum_{i=0}^{P-1} |p_i|^2] \end{aligned}$$

Recognizing that the MSE cost at a global setting is zero and also that $\theta = 0$ for the MSE cost, the change in MSE cost due to a sparse tapped delay line is upper bounded (due to optimality) by

$$\Delta J_{MSE|sparse} = \sigma_s^2 \sum_{i=0}^{P-1} |p_i|^2 \quad (17)$$

Compare (17) with (14); when the p_i are small, the cubic and quartic contributions of (14) are negligible and the quadratic term dominates. In this case, (14) is approximately a scaled version of (17),

$$\Delta J_{CM|QAM|sparse} \approx (4\sigma_s^2 - 2\sigma_s^2\kappa_s) \cdot \Delta J_{MSE|sparse} \quad (18)$$

which suggests a small deformation in both error surfaces due to a sparse tapped delay line, so the sparse CM settings stay in a tight neighborhood of the sparse and full-length Wiener settings. The MSE performance of the sparse CM receiver processing QAM data may therefore be approximated by $(1/(4\sigma_s^2 - 2\sigma_s^2\kappa_s)) \cdot (14)$.

C. Receiver Examples

To demonstrate on a practical signalling environment, we evaluate $(1/(4\sigma_s^2 - 2\sigma_s^2\kappa_s)) \cdot (14)$ and (17) for the $T/2$-spaced microwave channel model number 3 from the database at **http://spib.rice.edu**. Using 16-QAM signalling, the set $\mathcal{A}$ is chosen as the largest M coefficients in magnitude from the length-N Wiener setting found according to (3) and (8) with $N = 300$, which achieves perfect equalization. Figure 4 shows the MSE of the CM receiver in solid and the MSE receiver in circles, both versus the number of sparse coefficients.

The MSE performance may be referenced to the dashed line corresponding to a MSE for which CMA is typically transferred to a DD mode (about $10 - 20\%$ error rate). Observe

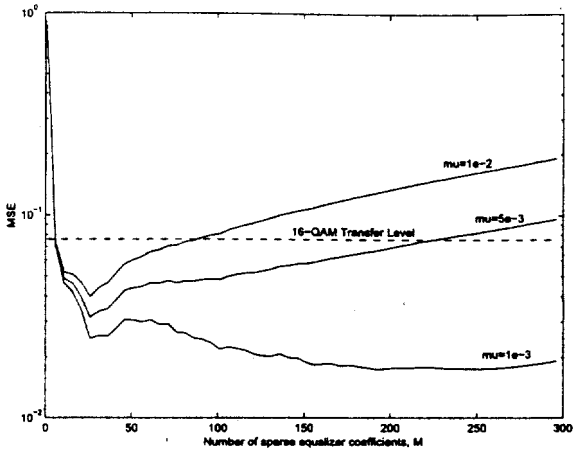

Figure 5: MSE performance including EMSE term from non-vanishing stepsize of sparse CMA versus the number of equalizer parameters.

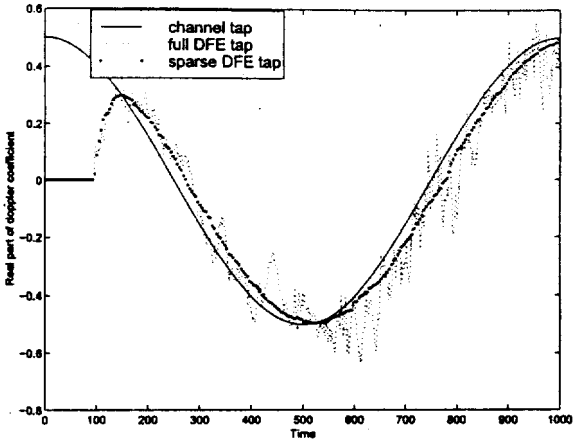

Figure 6: Simulation results showing time-varying channel coefficient and equalizers' tracking response for sparse and full-length DFE's.

that only a handful of sparse equalizer coefficients are required to reach the threshold – far fewer than that needed for perfect equalization. Also note that the MSE performance for the CM and MSE receivers is essentially identical. This implies that the sparse CM and MSE minima stay in a close neighborhood of the "full-length" Wiener setting. Also compare this figure to that in [1], which considers MSE performance of a CM receiver when the equalizer coefficients are constrained to be contiguous – the target threshold is reached with fewer sparse coefficients than contiguous coefficients.

D. Excess MSE

When the source is multi-modulus, the instantaneous CMA update term is generally non-zero, which causes a "rattling around" in the CM local minima. This behavior introduces an extra component to the error seen at the output of the CM receiver, referred to as *excess MSE* (EMSE). By solving a Lyapunov equation, [3] well approximates the EMSE of CMA in the absence of noise as

$$J_{CMA|EMSE} = \mu M \frac{\frac{E\{|s|^6\}}{(\sigma_s^2)^3} - \kappa_s^2}{2(3-\kappa_s)} (\sigma_s^2)^2 \sigma_r^2 \qquad (19)$$

where σ_r^2 is the power of the received signal and μ is the stepsize that controls equalizer parameter update. This result depends on the number of equalizer coefficients, which suggests: (i) the equalizer should be chosen long enough to mitigate ISI, but not too long so as to increase the EMSE; and (ii) a sparse equalizer can have better tracking capabilities compared to a full-length equalizer.

We approximate the MSE of a sparse equalizer updated with CMA by $(1/(4\sigma_s^2 - 2\sigma_s^2\kappa_s)) \cdot (14) + (19)$. This approximation is plotted in Figure 5 for various stepsizes. This figure illustrates that a more-dense sparse equalizer (large M/N) does not necessarily out-perform a less-dense sparse equalizer (small M/N).

IV. Performance Examples

A. Simulation Results

To illustrate the superior tracking capabilities of a sparse equalizer, a computer simulation is performed using the LMS algorithm with trained, 64-QAM data. The channel model is time-varying and is described by

$$c(z) = 1 + \alpha e^{jk\omega} z^{-\Delta} \qquad (20)$$

with $\alpha = 0.5$, $\omega = 2\pi/1000$, $\Delta = 47$, and k denotes a baud iteration. This single-echo multipath channel models a doppler phase roll. A decision feedback equalizer (DFE) with no forward filter and feedback filter of length $N = 47$ is used. Both a full-length DFE and a sparse DFE are tested. The sparse DFE has $M = 1$ active equalizer parameter at position 47 in the feedback filter.

Figure 6 shows the trajectories of the real parts of the channel coefficient, sparse equalizer coefficient, and full-length equalizer coefficient, each at position 47. The stepsize is changed from zero to $\mu = 1 \times 10^{-3}$ at $k = 100$ for both the sparse and full-length equalizers. The trajectory of the channel coefficient is denoted by the solid line, the trajectory of the sparse equalizer is denoted by the filled circles, and the trajectory of the full-length equalizer is denoted by the dotted line.

Observe from Figure 6 that the sparse equalizer has a far-smoother trajectory compared to the full-length equalizer. This is due to the lower EMSE of the sparse equalizer compared to the full-length equalizer. The reduction in EMSE can enable the use of a higher stepsize so that a sparse equalizer is able to track rapid time variations that a full-length equalizer cannot.

B. ASIC Results

The NXT-2000 is a high speed demodulator ASIC capable of receiving 8-VSB (vestigial sideband) or 64/256-QAM (quadrature amplitude modulation) signals. VSB is used in the US for high definition television (HDTV) signals over terrestrial broadcast and QAM is used for cable transmission. The NXT-2000 employs a sparse decision feedback equalizer that

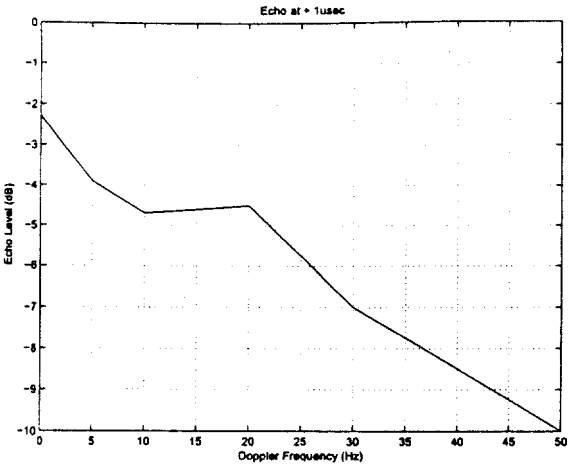

Figure 7: Laboratory results of the NXT-2000 demodulator showing echo level versus doppler frequency. The multipath echo is at $+1\mu sec$.

is blindly initialized with a linear IIR loop (see [2]). A modification of CMA is used to blindly update the linear IIR loop. The NXT-2000 uses a proprietary parameter allocation algorithm to dynamically place the sparse parameters in the correct positions of the forward and feedback filters. Other features of this ASIC can be found in [9]. The sparse equalizer significantly reduces chip area and power consumption while enhancing dynamic multipath performance. For example, the NXT-2000 typically dissipates about 1.25 watts of power for VSB reception, which is significantly less than other ASIC's that claim similar performance.

To demonstrate the dynamic tracking capabilities of the NXT-2000, laboratory experiments were conducted using a VSB modulator and multipath impairment generator which adds multipath at RF (approximately 500 MHz). The multipath is a single echo at $+1\mu sec$ that undergoes a doppler phase roll. (The VSB data rate is approximately 10.76 Megabaud.) The amplitude of the echo is increased until Threshold of Visibility (TOV) is reached, which corresponds to about 3×10^{-6} MPEG error rate performance. These tests are summarized in Figure 7 by plotting echo level versus doppler frequency.

Since indoor HDTV reception is unlikely to see greater than 20 Hz doppler shifts, the automatic gain control (AGC) circuitry is set to a loop bandwidth of about 20 Hz. Figure 7 shows better than -5 dB echo performance within 20 Hz doppler frequencies. However, for greater than 20 Hz doppler frequencies, the demodulator suffers a degredation in echo level. This roll-off is primarily due to the AGC loop bandwidth. We believe that the superior tracking capabilities of the NXT-2000 are due in large part to sparse equalization.

V. Concluding Remarks

A. Conclusions

We have studied the feasibility of using a sparse equalizer by removing the constraint that equalizer parameters be placed contiguously in the tapped delay line. We have shown that both the MSE and CM cost functions can admit sparse minima settings in near proximity to the full-length Wiener settings. Also, we have shown that a sparse equalizer can outperform a "full-length" equalizer.

B. Future Work

This paper has demonstrated the utility of implementing a sparse equalizer by showing the existence of CM and MSE settings that can provide acceptable MSE performance. However, much work remains in providing theoretical proof and practical guidelines for applications of sparse equalizers. For example, some areas of research regarding sparse equalization include

- Develop adaptive methods for equalizer parameter placement.
- For a given equalizer parameter placement method, analyze and prove stability and convergence.
- For a given equalizer parameter placement method, provide a description of tracking capabilities.
- For a given class of channels, establish design guidelines for sparse equalizer lengths and density, i.e., for M and N.
- Given a channel model, find a closed form expression or approximation for the optimum set of parameter positions, $\mathcal{A}$.
- Extend the robustness properties of common equalization update algorithms, such as CMA, to sparse equalizers. (Note that this paper extends CMA's robustness to undermodeling for a sparse equalizer.)

References

[1] T. J. Endres, B. D. O. Anderson, C. R. Johnson, Jr., M. Green, "Robustness to Fractionally-Spaced Equalizer Length using the Constant Modulus Criterion," *IEEE Trans. on Signal Processing*, vol. 47, no. 2, pp. 544-548, Feb. 1999.

[2] T. J. Endres, et al., "Carrier Independent Blind Initialization of a DFE," *IEEE Signal Processing Workshop on Signal Processing Advances in Wireless Communications*, Annaplois, MD, pp. 239-242, May. 1999.

[3] I. Fijalkow, C. E. Manlove, C. R. Johnson, Jr., "Adaptive Fractionally Spaced Blind CMA Equalization: Excess MSE," *IEEE Trans. on Signal Processing*, vol. 45, no. 1, pp. 56-66, Jan. 1998.

[4] D. N. Godard, "Self-Recovering Equalization in Two-Dimensional Data Communication Systems," *IEEE Transactions on Communications*, vol. 28, no. 11, pp. 1867-1875, Oct. 1980.

[5] C. R. Johnson, Jr., et al., "Blind Equalization Using the Constant Modulus Criterion: A Review," *Proc. of the IEEE*, Vol. 86, no. 10, pp. 1927-1950, Oct. 1998.

[6] C. R. Johnson, Jr., et al., "Fractionally-Spaced Equalizer Design for Digital Microwave Radio Channels," *Asil. Conference on Signals, Systems and Computers*, Pacific Grove, CA, pp. 290-294, Oct. 1995.

[7] Y. Li, Z. Ding, "Global Convergence of Fractionally-Spaced Godard (CMA) Adaptive Equalizers," *IEEE Trans. on Signal Processing*, vol. 44, no. 4, pp. 818-826, April 1996.

[8] Y. Li, K. J. Ray Liu, "Static and Dynamic Convergence Behavior of Adaptive Blind Equalizers," *IEEE Trans. on Signal Processing*, vol. 44, no. 11, pp. 2736-2745, Nov. 1996.

[9] P. Mannion, "IC cracks the code to improved digital TV reception," *Electronic Design*, pp. 35-39, August 23, 1999.

[10] J. R. Treichler, M. G. Larimore, "Thinned Impulse Responses for Adaptive FIR Filters," *International Conference on Acoustics, Speech and Signal Processing*, pp. 631-634, May 1982.

[11] J. R. Treichler and B. G. Agee, "A New Approach to Multipath Correction of Constant Modulus Signals," *IEEE Transactions on Acoustics, Speech, and Signal Processing*, vol. ASSP-31, no. 2, pp. 459-472, April 1983.

EUSIPCO 2000 (FINLAND)

On AR equalization with the Constant Modulus criterion

Azzédine Touzni†, Lang Tong‡, Raúl Casas†, C. Richard Johnson, Jr.‡
†NxtWave Communications, Langhorne, PA 18901
‡School of Electrical Engineering, Cornell University, Ithaca, NY 14853

Abstract— **This work studies the CM criterion applied to channel equalization with AR receivers. It is motivated by recently proposed blind IIR algorithms [6], [7], but may also be used for initializing a blind adaptive DFE. Blind IIR equalization is of practical interest for two main reasons: the IIR structure not only provides a parsimonious representation of a linear receiver, but may also be used for switching to DFE mode. We begin by showing that, unlike the FIR case, AR-CM receivers are equivalent to Wiener receivers for Gaussian sources. For sub-Gaussian input signals, however, due to the requirements of causality and stability of the receiver, characterization of CM solutions appears to be a complex problem. Thus, for sub-Gaussian sources, analysis is restricted to the special case of a MA(1) channel and AR(1) equalizer. Nevertheless, this study provides insight into the properties of AR-CM receivers by making the connection to the popular IIR-MMSE receivers.**

Keywords— **Constant Modulus Algorithm, IIR filtering, DFE**

1. Background and Motivation

This paper addresses the problem of blind equalization of finite impulse response (FIR) channels via autoregressive (AR) filters based on the Constant Modulus (CM) criterion [2], [4]. This equalization scheme is a special case of the more general framework of blind infinite impulse response (IIR) equalization recently proposed in [6], [7], [11], [12]. Blind IIR equalization is of practical interest for two main reasons: First or all, the IIR structure may provide a parsimonious representation of a linear receiver for a given channel. Furthermore, blind IIR equalization serves as an attractive initialization scheme for blind adaptive decision feedback equalizers (DFE).

FIR equalization based on the CM criterion has been extensively studied (see for instance [8], [9], [10]). However, little is known about IIR equalization based on the CM criterion beyond the update algorithm viewpoint. Unfortunately, the analysis in [5] is not applicable to this scenario due to the requirements of causality and stability of the receiver. The difficulty in analyzing the CM cost function for arbitrary channels, input signals and IIR equalizers restricts our focus to two separate cases. First we investigate CM solutions for Gaussian sources, finite impulse response (FIR) channels and AR receivers. AR-CM receivers for Gaussian sources are unique and equivalent to Wiener receivers, which is not true in the FIR case. Next we consider the characterization of minima for sub-Gaussian sources in the simplified case involving a noiseless MA(1) channel and an AR(1) equalizer. The aim is to provide insight towards answering interesting questions such as:

- What are the effects of the input signal distribution on location of CM receivers?
- Does the CM cost function admit multiple minima in the domain of stability of the receivers?
- How do CM receivers perform with respect to MMSE receivers?

Organization: Data model and MMSE/CM receiver definitions are introduced respectively in Sections 2 and 3. In Section 4, we characterize the minima (*i.e.* the receivers) of the CM cost function for Gaussian sources. Section 5 treats the case of sub-Gaussian sources for a simplified channel/equalizer setting. The conclusion discusses directions for future research on IIR-CM equalization.

A. Touzni (*touzni@nxtwavecomm.com*) is supported by INRIA (Institut National de Recherche en Informatique et Automatique), Rocquencourt, France and NxtWave Communications. L. Tong is supported by NSF Grant # CCR-9804019. R.A. Casas and C.R. Johnson, Jr. are supported in part by NSF Grant # ECS-9528363 and NxtWave Communications.

2. Data Model

We are interested in the estimation of an input signal $(s(n))_{n\in\mathbf{Z}}$ transmitted over a FIR channel from observations $(x(n))_{n\in\mathbf{Z}}$ given by

$$x(n) = \left[1+\sum_{k=1}^{N}\beta_k z^{-k}\right] s(n)+w(n) \quad (1)$$

$$= s(n)+\sum_{k=1}^{N}\beta_k s(n-k)+w(n) \quad (2)$$

where $\beta_k \in \mathbb{R}$ and $(w(n))_{n\in\mathbf{Z}}$ models noise. Estimates are given by a causal AR *receiver*

$$y(n) = \left[\frac{1}{1+\sum_{k=1}^{M}\alpha_k z^{-k}}\right] x(n) = -\sum_{k=1}^{M}\alpha_k y(n-k)+x(n) \quad (3)$$

where $\alpha_k \in \mathbb{R}$. In the sequel, we will use the polynomials $\beta(z) \stackrel{def}{=} 1+\sum_{k=1}^{N}\beta_k z^{-k}$ and $\alpha(z) \stackrel{def}{=} 1+\sum_{k=1}^{M}\alpha_k z^{-k}$. Let

$$\mathcal{Z}_\beta = \{\nu \in \mathbb{C} : \beta(\nu) = 0\} \quad (4)$$

be the set of channel roots. Here we assume there are no roots on the unit circle, *i.e.* $|\nu| \neq 1$ for all $\nu \in \mathcal{Z}_\beta$, and

that there are only simple roots. It is convenient to define the combined channel-equalizer transfer function $q(z) = \frac{\beta(z)}{\alpha(z)} = 1 + \sum_{k\geq 1} q_k z^{-k}$.

3. MMSE/AR-CM Receivers

The set of the Minimum Mean Square Error (MMSE) and AR-CM receivers are respectively defined as the minima of the following cost functions:

$$\begin{aligned} J_{\text{MMSE}}(\boldsymbol{\alpha}) &\stackrel{def}{=} \mathrm{E}\left[(y(n) - s(n))^2\right] \text{ and,} \\ J_{\text{CM}}(\boldsymbol{\alpha}) &\stackrel{def}{=} \mathrm{E}\left[\left(y(n)^2 - \rho\right)^2\right] \end{aligned} \tag{5}$$

where $\rho \stackrel{def}{=} \mathrm{E}\left[s^4\right]/\mathrm{E}\left[s^2\right]$ denotes the so-called ***dispersion*** constant used in the CM cost function [2], [4].

We introduce the following technical (but classical) assumptions: the input process $(s(n))_{n\in\mathbf{Z}}$, $s(n) \in \mathbb{R}$, is zero mean ($\mathrm{E}[s] = 0$), independent and identically distributed (i.i.d.). Under the necessary conditions $\mathrm{E}\left[s^2\right] < +\infty$ and $\mathrm{E}\left[s^4\right] < +\infty$ the input process is assumed to be either sub-Gaussian, *i.e.* $\kappa - 3 < 0$, or Gaussian, *i.e.* $\kappa = 3$, where κ is the kurtosis of the input signal defined by $\kappa \stackrel{def}{=} \mathrm{E}\left[s^4\right]/\mathrm{E}\left[s^2\right]^2$. The noise $(w(n))_{n\in\mathbf{Z}}$ is i.i.d., zero mean Gaussian noise of variance $\mathrm{E}\left[w^2\right]$, and is independent of the source.

Given $M \geq N$ [1], the Wiener receivers

$$\boldsymbol{\alpha}^{\dagger} \stackrel{def}{=} \arg\min_{\boldsymbol{\alpha}(z)} J_{\text{MMSE}}(\boldsymbol{\alpha}) \tag{6}$$

admit the solutions given by a spectral factorization of the received signal autocorrelation function (see (8) and (9) below). A less understood problem is the characterization of the CM receiver(s) defined by

$$\boldsymbol{\alpha}^{\star} \stackrel{def}{=} \arg\min_{\boldsymbol{\alpha}(z)} J_{\text{CM}}(\boldsymbol{\alpha}). \tag{7}$$

This question is investigated in the next sections.

4. Gaussian Sources

The structure of the AR receiver creates striking similarities and differences between FIR and AR receivers derived from the CM criterion for Gaussian sources. In the FIR case, Gaussian sources lead to a continuum of CM receivers which minimize output power (see [10]). Similarly, AR-CM receivers also minimize output power for Gaussian sources, yet they are unique (under certain length conditions) and equivalent to the Wiener receivers. This result is summarized in the lemma that follows.

Lemma *1:* Whenever $\kappa = 3$ and $M \geq N$ the CM cost function $J_{\text{CM}}(\boldsymbol{\alpha})$ has a unique global minimum which matches the Wiener solution. We have,

$$\boldsymbol{\alpha}^{\star}(z) = \boldsymbol{\alpha}^{\dagger}(z) = \boldsymbol{g}_{min}(z) \tag{8}$$

[1] When $M < N$ the MSE cost function may have multiple local minima [1].

where $\boldsymbol{g}_{min}(z)$ is the unique monic polynomial known as the spectral factor of the received signal autocorrelation function satisfying

$$\mathrm{E}\left[s^2\right]\boldsymbol{\beta}(z)\boldsymbol{\beta}^{*}(1/z^{*}) + \mathrm{E}\left[w^2\right] = \gamma^2 \boldsymbol{g}_{min}(z)\boldsymbol{g}^{*}_{min}(1/z^{*}) \tag{9}$$

where $\gamma^2 > 0$ is a scale factor.

Proof: See Appendix A.

Remark: In the noiseless case the unique minimum for the CM and Wiener criteria is given by

$$\boldsymbol{\alpha}^{\star}(z) = \boldsymbol{\alpha}^{\dagger}(z) = \boldsymbol{g}_{min}(z) = \prod_{\substack{\nu\in\mathcal{Z}_{\beta} \\ |\nu|<1}} (1 - \nu z^{-1}) \prod_{\substack{\nu\in\mathcal{Z}_{\beta} \\ |\nu|>1}} (1 - \frac{1}{\nu^{*}} z^{-1}). \tag{10}$$

5. Sub-Gaussian Sources

Characterization of AR-CM receivers for sub-Gaussian sources is significantly more complex due to the presence of high order statistics. For this reason we consider an academic noiseless MA(1) channel and AR(1) equalizer, *i.e.* $M = N = 1$. We denote $\beta_1 = \beta \in \mathbb{R}$, $\alpha_1 = \alpha \in \mathbb{R}$, $|\alpha| < 1$. Here, the combined channel-equalizer response is given by

$$\boldsymbol{q}(z) = \frac{1 + \beta z^{-1}}{1 + \alpha z^{-1}} = 1 + (\alpha - \beta)\sum_{k=1}^{\infty}(-\alpha)^k z^{-k}. \tag{11}$$

From above, the Wiener receivers have solutions $\alpha^{\dagger} = \beta$ when $|\beta| < 1$ (noiseless minimum phase channels) and $\alpha^{\dagger} = 1/\beta$ when $|\beta| > 1$ (noiseless maximum phase channels). For Gaussian sources CM receivers match the Wiener receivers, *i.e.* $\alpha^{\star} = \alpha^{\dagger}$ when $\kappa = 3$.

To characterize the CM receivers in the sub-Gaussian case, we express the CM cost function in terms of the channel-equalizer impulse response as

$$\begin{aligned} J_{\text{CM}}(\alpha) \;=\; & (\kappa - 3)\mathrm{E}\left[s^2\right]^2 \|q\|_4^4 \\ & + 3\mathrm{E}\left[s^2\right]^2 \|q\|_2^4 - 2\rho\mathrm{E}\left[s^2\right]\|q\|_2^2 + \rho^2 \end{aligned} \tag{12}$$

where

$$\|q\|_2^2 = 1 + \frac{(\alpha-\beta)^2}{1-\alpha^2}, \quad \|q\|_4^4 = 1 + \frac{(\alpha-\beta)^4}{1-\alpha^4} \tag{13}$$

with the definition $\|q\|_p^p = 1 + \sum_{k\geq 1}|q_k|^p$. The straightforward way to investigate the minima of the CM cost function is based on the determination of the extrema (in the domain of stability of the receiver) and on the characterization of the convexity of the cost function at these solutions.

Extrema of $J_{\text{CM}}(\alpha)$ are solutions of

$$\begin{aligned} \frac{dJ_{\text{CM}}(\alpha^{\star})}{d\alpha} = 4(\alpha-\beta)\Bigg[& (\kappa-3)\mathrm{E}\left[s^2\right]^2 \frac{(\alpha-\beta)^2(\beta\alpha^3-1)}{(1-\alpha^4)^2} \\ & + 6\beta\mathrm{E}\left[s^2\right]^2 \frac{(\beta\alpha-1)(\alpha-\frac{1+\beta^2}{2\beta})}{(1-\alpha^2)^3} + \mathrm{E}\left[s^4\right]\frac{(\beta\alpha-1)}{(1-\alpha^2)^2}\Bigg] = 0 \end{aligned} \tag{14}$$

We study the solutions of (14) and their stability under the constraint $|\alpha^\star| < 1$ for either minimum-phase or maximum-phase channels.

Lemma 2: [2] For $|\beta| < 1$, $\alpha^\star = \beta$ is a unique extremum of $J_{\mathrm{CM}}(\alpha)$ in $|\alpha| < 1$ corresponding to a global minimum. The Hessian at this minimum

$$\frac{d^2 J_{\mathrm{CM}}(\alpha^\star)}{d\alpha^2} = 4\mathrm{E}\left[s^2\right]^2 \frac{\kappa - 3}{\beta^2 - 1} \tag{15}$$

is strictly positive.

For $|\beta| > 1$, there exists a solution in the interval $0 < \alpha^\star < \frac{1}{\beta^{1/3}}$ for $\beta > 0$ and $\frac{1}{\beta^{1/3}} < \alpha^\star < 0$ for $\beta < 0$. When $|\beta| \gg 1$ a closed-form solution and its corresponding Hessian are given respectively by

$$\alpha^\star = \frac{\kappa}{3\beta} + o(|\beta^{-1}|) \tag{16}$$

and

$$\frac{d^2 J_{\mathrm{CM}}(\alpha^\star)}{d\alpha^2} \simeq -12(\kappa - 3)\mathrm{E}\left[s^2\right]^2 \beta^4 > 0. \tag{17}$$

For minimum-phase channels $J_{\mathrm{CM}}(\alpha)$ admits a unique global minimum, identical to the Wiener solution, in the domain of stability of the receiver. Both CM and Wiener receivers achieve perfect estimation of the input signal for minimum phase channels. When the channel is maximum-phase Wiener and CM receivers are different. In this case, the location of the pole of the CM solution depends on the kurtosis of the input signal. These results are summarized in Table 1. Figure 1 plots CM cost functions for a minimum phase channel and also for a maximum phase channel. It appears to be difficult to extend this result (at least with this approach) for AR receivers of higher order since equations of the extrema do not admit general analytical solutions.

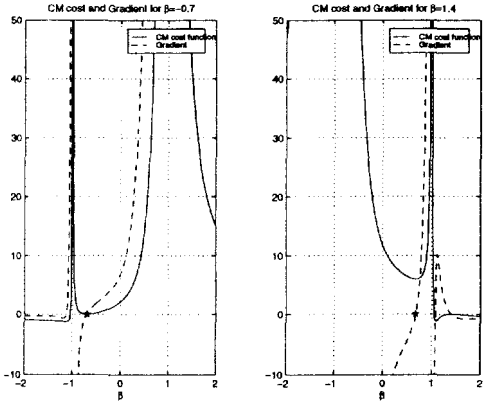

Fig. 1. CM cost and gradient for minimum phase (left) and maximum phase (right) channels and a constant modulus source.

The closed-form solution (16) is consistent with the results given in Lemma 1 for Gaussian input signals: when $\kappa \to 3$ we have $\alpha^\star \to \frac{1}{\beta}$. Figure 2 validates (16) by plotting the actual CM extrema achieved by a gradient technique and the approximate expression (16) for different values of κ.

[2]The proof is available on request.

	Gaussian	sub-Gaussian
$\lvert\beta\rvert < 1$	$\alpha^\star \stackrel{\circ}{=} \beta$	$\alpha^\star \stackrel{\circ}{=} \beta$
$\lvert\beta\rvert > 1$	$\alpha^\star \stackrel{\circ}{=} \frac{1}{\beta}$	$\lvert\beta\rvert \gg 1, \alpha^\star \simeq \frac{\kappa}{3\beta}$

TABLE 1

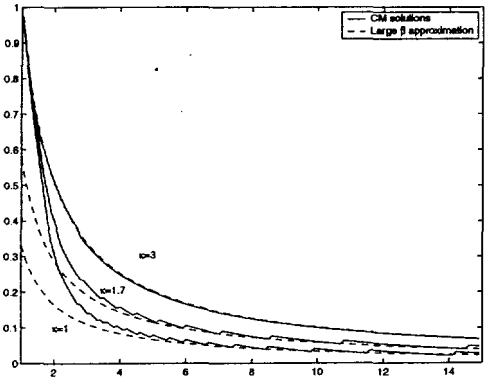

Fig. 2. CM exact minima and closed-form solution versus β for different κ.

Notice that for sub-Gaussian signals, CM and Wiener receivers result in different intersymbol interference (ISI) measured by $\mathrm{ISI}(\alpha) \stackrel{def}{=} \frac{\sum_{k=0}^{\infty} |q_k| - \max_k |q_k|}{\max_k |q_k|}$. For non-minimum phase channels we have

$$\mathrm{ISI}(\alpha^\dagger) \simeq \frac{2}{\beta} > \mathrm{ISI}(\alpha^\star) \simeq \frac{\kappa}{3\beta} \tag{18}$$

so the residual ISI given by the CM solution for AR equalization is always smaller or equal to the residual ISI given by the Wiener solution. The AR-CM filter can perform better than a Wiener filter in terms of ISI in spite of the fact that complete knowledge of the input data is never used by AR-CM as it is by AR-Wiener. The result is validated in Figure 3, where we compare the ISI for the Wiener and CM solutions as a function of β for several values of kurtosis κ.

5. Conclusion

We have investigated the performance of the CM criterion for AR receivers. Even though the data model is quite academic, we have presented several novel results that point out the differences between the AR-CM criterion and the FIR-CM criterion. In this particular case, we have shown that CM and Wiener receivers are equivalent for Gaussian sources, given the AR filter has at least the same number of parameters as the channel. For sub-Gaussian sources, and a simplified MA(1) channel and AR(1) filter, we have given solutions of the CM receiver and proven that

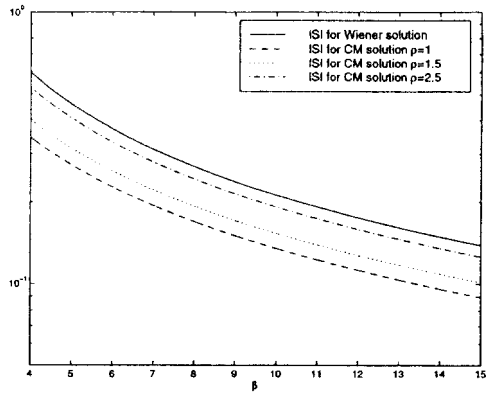

Fig. 3. Comparison of ISI for Wiener and CM solutions with AR equalizer structure ($\rho = \mathrm{E}\left[s^4\right]/\mathrm{E}\left[s^2\right]$).

the CM criterion does not admit spurious local minima in the domain of stability of the AR receiver for the mininum phase case. The extension of this work, *i.e.* the characterization of CM receivers, seems difficult for the general case of an ARMA receiver (at least from the analysis of the gradient of the CM cost function). Another problem of interest is the analysis of the convergence properties of the stochastic update gradient algorithm [6], [7], [12]. This blind adaptive IIR equalization problem parallels problems involving adaptive IIR algorithms for signal processing and control based on the least mean square algorithm (LMS) in the literature of the late 70's and early 80's [3].

Appendix A

Proof: Expand the MMSE cost function

$$J_{\mathrm{MMSE}}(\boldsymbol{\alpha}) = \mathrm{E}\left[y^2(n) - 2y(n)s(n) + s^2(n)\right]$$

and note that $y(n) = s(n) + \sum_{k=1}^{\infty} q_k s(n-k)$ which gives

$$J_{\mathrm{MMSE}}(\boldsymbol{\alpha}) \;=\; \mathrm{E}\left[y^2(n)\right] - \mathrm{E}\left[s^2(n)\right]$$

by independence of the source. Wiener solutions lead to the minimization of the output power. The sequence $(x(n))_{n\in\mathbf{Z}}$ with $x(n) = [\boldsymbol{\beta}(z)]s(n) + w(n)$ is a stationary Gaussian stochastic process that can be represented as $x(n) = [\boldsymbol{g}_{min}(z)]\varepsilon(n)$ where $(\varepsilon(n))_{n\in\mathbf{Z}}$ is a wide sense white Gaussian process of variance $\mathrm{E}\left[\varepsilon^2\right] = \gamma^2$. In [1] it is shown that when $M \geq N$, the output power cost function $\mathrm{E}\left[y^2\right]$ where $y(n) = [\frac{1}{\boldsymbol{\alpha}(z)}]x(n)$ has a unique global minimum $\boldsymbol{\alpha}^{\dagger}(z) = \boldsymbol{g}_{min}(z)$.

Next, we show that CM solutions also lead equivalently to the minimization of output power. For Gaussian sources $\mathrm{E}\left[s^4(n)\right] = 3\mathrm{E}\left[s^2(n)\right]^2$. Furthermore, the receiver output is also Gaussian and thus $\mathrm{E}\left[y^4(n)\right] = 3\mathrm{E}\left[y^2(n)\right]^2$. Expanding the CM cost function we find

$$J_{\mathrm{CM}}(\boldsymbol{\alpha}) = 3\mathrm{E}\left[y^2(n)\right]^2 - 6\mathrm{E}\left[y^2(n)\right]\mathrm{E}\left[s^2(n)\right] + 9\mathrm{E}\left[s^2(n)\right]^2$$

and set its gradient to zero to find solutions. We get

$$\nabla_{\boldsymbol{\alpha}} J_{\mathrm{CM}}(\boldsymbol{\alpha}) = 6\left(\mathrm{E}\left[y^2(n)\right] - \mathrm{E}\left[s^2(n)\right]\right)\nabla_{\boldsymbol{\alpha}}\mathrm{E}\left[y^2(n)\right] = 0.$$

Solutions $\boldsymbol{\alpha}^{\star}$ satisfy **i)** $\mathrm{E}\left[y^2(n)\right] = \mathrm{E}\left[s^2(n)\right]$ or **ii)** $\nabla_{\alpha}\mathrm{E}\left[y^2(n)\right] = 0$. Because $y(n) = [\boldsymbol{q}(z)]s(n) + [\frac{1}{\boldsymbol{\alpha}(z)}]w(n)$ in order to satisfy **i)** we must have $w(n) = 0$. Thus, in the noisy case **i)** cannot be achieved. In the noise free case, [1] shows that $\mathrm{E}\left[y^2\right] \geq \gamma^2 = \mathrm{E}\left[s^2\right]$ with equality when $\boldsymbol{\alpha}^{\star}(z) = \boldsymbol{g}_{min}(z)$, and furthermore, when $M \geq N$, that **ii)** yields a unique extremum, corresponding to the unique global minimum $\boldsymbol{\alpha}^{\star}(z) = \boldsymbol{g}_{min}(z)$. ■

References

[1] K.J. Aström, T. Söderström, "Uniqueness of the Maximum Likelihood estimates of the parameters of an ARMA model," *IEEE Transactions on Automatic Control*, vol. AC-19, no. 6, pp.769-773, November 1974

[2] D.N. Godard, "Self-recovering equalization and carrier tracking in two-dimensional data communication systems," *IEEE Transactions on Communications*, vol.28, no.11, pp.1867-1875, November 1980

[3] C.R. Johnson, Jr., M.G. Larimore, J.R. Treichler, B.D.O. Anderson, "SHARF convergence properties," *IEEE Transactions on Circuits and Systems*, vol. 28, no. 6, pp.499-510, June 1981

[4] J.R. Treichler and B.G. Agee, "A new approach to multipath correction of constant modulus signals," *IEEE Transactions on Acoustics, Speech and Signal Processing*, vol. ASSP-31, no.2, pp.459-72, April 1983

[5] G.J. Foschini, "Equalization without altering or detecting data", *ATT Tech. Journal*, vol. 64, pp. 1885-1911, October 1985.

[6] C.A. Faria da Rocha, O. Macchi, "A novel self-learning adaptive recursive equalizer with unique optimum for QAM," *Proc. IEEE International Conference on Acoustics, Speech and Signal Processing*, Adelaide, Australia, pp.481-484, April 1994

[7] F.R.P. Cavalcanti, J.C.M. Mota, "Predictive blind equalization with the constant modulus criterion," *Proc. IEEE Signal Processing Workshop on Signal Processing Advance in Wireless Communications*, Paris, France, pp.49-52, April 1997

[8] I. Fijalkow, A. Touzni, J.R. Treichler, "Fractionaly-spaced equalization using CMA: Robustness to channel noise and lack of robustness," *in IEEE Transactions on Signal Processing*, vol. 45, No. 1, pp. 56-66, January 1997

[9] H.H. Zeng, L. Tong and C.R. Johnson, Jr., "Relationships between the constant modulus and Wiener receivers," *IEEE Transactions on Information Theory*, vol. 44, no. 4, pp.1523-38, July 1998

[10] C.R. Johnson, Jr, P. Schniter, T.J. Endres, J.D. Behm, D.R. Brown, R.A. Casas, "Blind equalization using the constant modulus criterion: a review," *Proceedings of the IEEE*, vol. 86, no. 10, October 1998, pp.1927-1950

[11] J. Labat, O. Macchi, C. Laot, "Adaptive decision feedback equalization: can you skip the training period?" *IEEE Transactions on Communications*, vol.46, no.7, pp.921-930, July 1998

[12] T.J. Endres, S.N. Hulyalkar, T.A. Schaffer, C.H. Strolle, "A constant modulus decision feedback equalizer," *United States Patent*, Patent no. 60,148,983, August 1999.